

UNIVERSITY OF OKLAHOMA

GRADUATE COLLEGE

CARBOXYLIC ACID KETONIZATION ON ZEOLITES

A THESIS

SUBMITTED TO THE GRADUATE FACULTY

in partial fulfillment of the requirements for the

Degree of

MASTER OF SCIENCE

By

MANASA GODAVARTHY

Norman, Oklahoma

2016

CARBOXYLIC ACID KETONIZATION ON ZEOLITES

A THESIS APPROVED FOR THE  
SCHOOL OF CHEMICAL, BIOLOGICAL AND MATERIALS ENGINEERING

BY

---

Dr. Steven Crossley, Chair

---

Dr. Daniel Resasco

---

Dr. Lance Lobban

© Copyright by MANASA GODAVARTHY 2016  
All Rights Reserved.

## **Acknowledgements**

I am grateful for Dr. Steven Crossley being my advisor for Master's Program research work. He is a very passionate toward this work and his encouragement and enthusiasm helped me a great deal in getting inquisitive about research.

Dr. Daniel Resasco is an amazing personality and I could experience about how inspiring professors can be to students. I am grateful to be associated with Dr. Lance Lobban, one of the very warm people I came across in life, and with Dr. Tawan Sooknoi for the knowledge he shares with us on his summer visits to OU.

I am very happy for being a part of this group where ideas are continuously exchanged and students are encouraged to think and constantly mentored for being professionals in the real world scenario.

I would like to specially appreciate Abhishek for mentoring me during my first semester here and for the patience he showed in answering some very random questions in research related work. I am thankful for the great friend he is, his presence in my life and for the support he was in the past 8 years of my life.

My special thanks to

- the friends I made here - Taiwo, Daniel Santharaj , Nick, Rajiv, Yen, Lei and Tuong who made my life on a foreign land easier and happier,
- the officers of the Chemical Engineering Graduate society Reda, Nhung and Sweta for the fun team we made and the events we organized,
- all other graduate students in the OU biofuel group who were a part of my life here, helping me on and off work.

I want to specially acknowledge the funding source for my work ACS PRF and the University of Oklahoma for providing me with the opportunity to study and perform this research and contribute to science.

Most importantly, I would like to thank my parents for raising me to be such an independent thinker and a self-made person and my kid brother who has always been my best friend and confidante. I am grateful for all the support from my extended family and the inspirational women in my family who contributed their share to the betterment of education in India.

## Table of Contents

Acknowledgements.....	iv
List of Tables .....	viii
List of Figures .....	ix
<b>1. Chapter 1: Introduction and Literature .....</b>	<b>1</b>
<b>1.1. Catalysts.....</b>	<b>3</b>
<b>1.1.1. H-ZSM 5.....</b>	<b>3</b>
<b>1.1.2. HY .....</b>	<b>3</b>
<b>1.1.3. H-Beta .....</b>	<b>4</b>
<b>1.2. Current understanding of the Mechanism.....</b>	<b>4</b>
<b>1.3. Previous work in our group[40] .....</b>	<b>9</b>
<b>1.4. Research Objectives .....</b>	<b>11</b>
<b>2. Chapter 2: Experimental set up .....</b>	<b>13</b>
<b>2.1. Catalyst Preparation .....</b>	<b>13</b>
<b>2.2. Flow reactor and conditions .....</b>	<b>13</b>
<b>2.3. TPD experiments – set up and conditions.....</b>	<b>14</b>
<b>2.3.1. IPA - TPD experiment setup .....</b>	<b>14</b>
<b>2.3.2. TPD experiment setup .....</b>	<b>15</b>
<b>2.3.3. Pulsing experiments with two acids and TPD.....</b>	<b>16</b>
<b>2.4. BET experiments – Set up and experiment .....</b>	<b>16</b>
<b>2.5. XRD experimental setup .....</b>	<b>17</b>

2.6.	SEM experimental set up .....	17
3.	Chapter 3 : Results and Discussion .....	18
3.1.	Pivalic acid .....	18
3.2.	Benzoic acid and <sup>13</sup> C labelled benzoic acid.....	23
3.2.1.	Co-feeding acetic acid and Benzoic acid.....	26
3.2.2.	Carbon Labelled experiments.....	30
3.3.	Propionic acid.....	32
3.4.	Hexanoic acid .....	38
3.4.1.	Different catalysts .....	40
3.5.	Mesoporous catalyst .....	41
3.5.1.	Preparation of Parent zeolite .....	42
3.5.2.	De-silication to produce mesopores .....	43
3.5.3.	Acid wash to clean the mesoporous parent zeolite .....	43
3.5.4.	Characterization results of the three zeolites.....	44
3.5.5.	Flow reactions results .....	48
3.6.	Succinic acid .....	50
3.7.	Furoic acid.....	52
4.	Chapter 4: Conclusions.....	54
5.	References.....	55

## List of Tables

Table 1: Synthesized Mesopore series characterization SEM results for crystal size .	43
Table 2: BET results showing micro-porosity, mesoporosity and surface area.....	46
Table 3: IPA-TPD results for the Mesoporous Series of Zeolites .....	48
Table 4: Table showing various solvents, molar ratios and temperatures used for succinic acid flow reactions .....	51



## List of Figures

Figure 1 : General schematic of ketonization mechanism .....	2
Figure 2: Proposed mechanism for ketonization of carboxylic acid over ZrO <sub>2</sub> catalyst [35].....	6
Figure 3: selectivity of propionic acid reactions in HZSM5 and HT zeolites[34].....	7
Figure 4: Proposed ketonization mechanism of acetic acid on HZSM-5 by Chang et al showing dehydroxylation of zeolite [36].....	8
Figure 5: Acetic acid TPD on HZSM-5 showing an initial dehydration step involved in the reaction pathway[40] .....	10
Figure 6 : Proposed mechanism of ketonization over zeolites [40] .....	11
Figure 7: Graph showing selectivity towards ketone formation in reaction of 4 acids with decreasing number of alpha hydrogens on three different oxide catalysts[20]	18
Figure 8: Experimental results with labelled acetic acid and Pivalic acid reactions over Titania reported in literature [20].....	19
Figure 9: Flow reaction studies with Pivalic acid showing conversion and selectivity with varying reaction temperatures at constant W/F = 0.041.....	20
Figure 10: Flow reaction comparison between acetic acid ketonization vs ketonization of acetic acid when co-fed with Pivalic acid (molar ratio = 1: 5) at T=300°C and W/F =0.3 w.r.t. acetic acid .....	22
Figure 11: Pivalic acid TPD on H-ZSM5 showing decomposition into isobutylene, water and CO <sub>2</sub> .....	23
Figure 12 : Benzoic acid TPD on H-ZSM5 showing an initial dehydration step involved in the mechanism.....	25
Figure 13: Flow reaction studies co-feeding acetic acid with benzoic acid (molar ratio = 1:8) at T=300C and W/F =0.22, showing formation of two ketones.....	28
Figure 14 a, b: Benzoic acid TPD studies pulsing in acetic acid on benzoyl adsorbed HZSM5 showing acetophenone and acetone respectively .....	29

Figure 15 a, b: Benzoic acid TPD studies pulsing in acetic acid on <sup>13</sup> C labelled benzoyl adsorbed HZSM5 showing acetophenone and acetone respectively.....	31
Figure 16 : Flow reaction studies of propionic acid co fed with acetic acid in a molar ratio 1:1 and W/F = 0.3 w.r.t acetic acid at T=300C .....	33
Figure 17: Flow reaction studies of propionic acid co fed with acetic acid in a molar ratio 1:1 and W/F = 0.3 w.r.t acetic acid at T=315C .....	34
Figure 18: Flow reaction studies of propionic acid co fed with acetic acid in a molar ratio 1:1 and W/F = 0.3 w.r.t acetic acid at T=325C .....	34
Figure 19: TPD experiment of propionic acid showing dehydration on the catalyst surface with increasing temperature .....	35
Figure 20: TPD experiment of propionic acid showing desorbing hydrocarbons with increasing temperature .....	36
Figure 21: TPD experiment of Pentanone showing water desorbing at higher temperature confirming aldol condensation during propionic acid TPD .....	37
Figure 22: TPD experiment of Pentanone showing hydrocarbons confirming aldol condensation during propionic acid TPD.....	38
Figure 23: Flow reaction studies of hexanoic acid co fed with acetic acid at T=300C over HZSM-5 showing cross ketone as a primary product with very low partial pressures of hexanoic acid .....	39
Figure 24: Flow reaction results of hexanoic acid co fed with acetic acid (molar ratio = 1 : 10) at T=300C over HZSM-5, H-Beta and HY showing TOF for cross ketone.....	40
Figure 25: Flow reaction results of hexanoic acid co fed with acetic acid at T=300C over HZSM-5, H-Beta and HY showing TOF for self-ketone of Hexanoic acid.....	41
Figure 26 : SEM of the synthesized parent zeolite sample showing a crystal size of 10 micron .....	44
Figure 27: SEM image of the mesoporous zeolite sample .....	45
Figure 28 : SEM image of the acid washed mesopore sample .....	45
Figure 29: XRD of the parent zeolite and mesoporous zeolite showing crystallinity .	47

<b>Figure 30: Turnover frequencies for cross ketone on two different catalysts in co-feeding experiments of hexanoic acid with acetic acid (molar ratio = 1 : 10) at T=300C .....</b>	<b>49</b>
<b>Figure 31: Turnover frequencies of mesoporous series based on conversion of hexanoic acid co fed with acetic acid to a cross ketone at T=300C and same conditions compared to commercial H-ZSM5.....</b>	<b>50</b>
<b>Figure 32: TPD results of succinic acid on H-ZSM5 with acetic acid as solvent .....</b>	<b>52</b>
<b>Figure 33: TPD results of 2-Furoic acid over H-ZSM5 with acetic acid as solvent.....</b>	<b>53</b>

## 1. Chapter 1: Introduction and Literature

Carboxylic acids present in crude oil result in considerable corrosion problems for petroleum refiners. Typically, carboxylic acids containing one or more saturated five or six membered ring structures are termed as naphthenic acids. Crude oil contains almost up to 4 wt.% naphthenic acids and it may vary [1]. The acids pose a significant threat to refineries, the corrosive nature of these acids being the damaging factor. Caustic treatment of crude oil to eliminate the acid content is not ideal for reasons like subsequent waste water treatment or emulsion formations. These challenges increased the efforts towards finding alternative methods like catalytic treatment of the acids [2-4]. As depletion of resources is a challenge due to the increasing the crude oil demand, bio-oil is a renewable source of energy.

Bio-oil is a large resource for renewable energy in the country and extensive research is going on about the production and upgradation of bio-oil for few decades now. Fast pyrolysis of bio mass contains significant amounts phenolics, furanics, carboxylic acids and light oxygenates [5-12]. Research in our group focuses on developing methods to eliminate the oxygen content and retain the carbon and overcoming certain challenges involved in these processes. These acids are corrosive, may promote polymerization in these streams and deactivate the catalyst [5-18]. The conversion of these acids to stable species is desired.

One reaction that is promising and has gained a lot of interest is the ketonization reaction [19-22]. As shown in the figure 1, two carboxylic acids react to form a ketone,

CO<sub>2</sub> and H<sub>2</sub>O. Unlike the acid, ketone is not corrosive. This reaction could be an effective way to convert unwanted acids in the crude oil or bio-oil streams. These ketones can be studied to undergo aldol condensation/hydrogenation to produce larger carbon chain hydrocarbons [21, 23, 24].

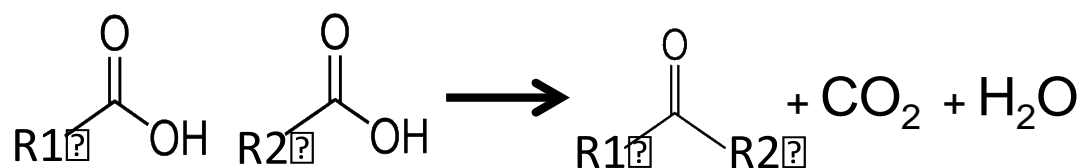


**Figure 1 : General schematic of ketonization mechanism**

Better understanding of the mechanism behind the conversion of carboxylic acids into ketones could lead to improvements in catalyst design for the processing of problematic crude/bio-oils. The ketonization reaction is reported to be observed over zeolites and H-ZSM5 is one of the commonly used catalysts in refineries, so a deep understanding of the mechanism of the ketonization reaction over zeolites is needed for application. However, very few studies on this topic exist in literature.

Also, studies on this reaction are subject to some controversy regarding the mechanism of ketonization on heterogeneous catalysts [25]. Investigating the reaction and the reaction intermediates on zeolite catalyst can help in understanding the reaction mechanism.

## **1.1. Catalysts**

Zeolites are microporous crystalline structures made of silicon, aluminum and oxygen forming a framework with channels and cavities. Tetrahedral silica and alumina are basic building blocks of the structure, where the Si or Al (T atom) is the center and oxygen is at four corners of the tetrahedron[26]. Each oxygen is shared between two T atoms, neutralizing the +4 oxidation state Si atom and giving a negative charge to the +3 oxidation state Al atom. This negative charge can be balanced by a proton to form a Brønsted acid site (BAS). Zeolites are widely used in a variety of ways in industrial catalytic applications.

### **1.1.1. H-ZSM 5**

ZSM-5 catalyst was first synthesized by Argauer and Landolt in 1969[27]. This zeolite is widely used in the petroleum industry as a heterogeneous catalyst for cat cracking and isomerization reactions. ZSM-5 has the framework type MFI and is a medium pore zeolite with channels defined by ten-membered rings. The pore diameter is about 5Å. The zeolite used for the experiments is a commercial catalyst (CBV 8014) purchased from Zeolyst International in ammonium form with a Si/Al ratio of 40. Here on the catalyst would be referred as H-ZSM5.

### **1.1.2. HY**

HY is a catalyst that is used for fluid catalytic cracking reactions in the petroleum industry. The Y zeolite has a Faujasite framework and consists of two types of cages, the

sodalite cage and the supercage. The supercage is enclosed in between 10 sodalite cages and can be accessed from 4 windows. It is a large pore zeolite where each pore is formed by a 12 membered ring with a relatively large diameter of about 7 Å [27, 28].

Commercial HY zeolites with Si/Al ratios of 2.6 and 40 (CBV 600 and CBV 780) were purchased from Zeolyst international in the hydrogen cation form for the reactions in this study.

### **1.1.3. H-Beta**

Zeolite Beta has a BEA framework. Beta zeolite that contains a three directional 12 membered ring channel system with pore dimensions of about 6.7 Å [29]. It is a large pore zeolite where each pore is formed by a 12 membered ring.

Commercial Zeolite Beta with a Si/Al ratio of 19, was purchased from Zeolyst international in its ammonium form as CP814C.

## **1.2. Current understanding of the Mechanism**

Ketonization reaction has been studied for over three decades, on salts, metal oxides and more recently over zeolites. Several mechanisms were proposed from observations over salts such as decarboxylation and nucleophilic attack, a concerted mechanism involving two mono-dentate carboxylates and coupling of two carboxylates bound to the same cations.

In heterogeneous catalysis, most of the work was done over metal oxides and several proposed mechanisms and surface intermediates exist. Ample literature is available

about mechanism of the ketonization reaction of acids on reducible metal oxides proposing various reaction intermediates like ketene like species, and  $\beta$ -keto acids[21, 25].

In the work by Ponec et al., [14, 19, 20, 30] over metal oxide catalysts, experimental observations indicated that the acid molecule that loses its alpha hydrogen subsequently upon producing the ketone, loses  $\text{CO}_2$ . They performed  $^{13}\text{C}$  labelled experiments that confirmed that the alpha hydrogen containing acid molecule loses  $\text{CO}_2$  after producing a ketone. Over iron oxide, vanadia and titania catalysts, it has been observed that, the selectivity for ketonization decreased with reduced number of alpha hydrogens, tri methyl substituted acids containing no alpha hydrogen produced no measurable amounts of ketone. One of the explanations for these results could be the steric hindrance due to the methyl groups that inhibits ketone formation. However, ketonization is not observed by coupling two molecules of benzoic acid, which is less bulky than methyl substituted acids. So, ruling out steric hindrance as the reason, they concluded that the presence of alpha hydrogen is necessary for ketone formation. This result is contradicting to earlier reported results of 2,2,5,5, tetra methyl adipic acid, which lacks alpha hydrogen forms a ketone over BaO and KF[31]. The importance of alpha hydrogen still needs to be studied for understanding the mechanism over different families of catalysts.

A ketene species has been observed experimentally by several groups and it has been speculated that ketene is the intermediate in the ketonization mechanism on oxides [30,



32]. Literature also reports the formation of a ketone and CO<sub>2</sub> from decarboxylation of a β-keto acid over metal oxides [21]. A β-keto acid is an organic compound containing a ketone group in the second carbon / β position from the carboxylic acid group. The formation of a β-keto acid is reported as the attack of an enolated species on an adsorbed carboxylate on the catalyst surface. A pathway proposed by Renz et al., suggests that the β-keto acid results from the coupling of an acyl ion and a surface enolate, figure 2 shows the mechanism [33]. They propose that decomposition of the acid is the rate determining step which was debated in the later studies.

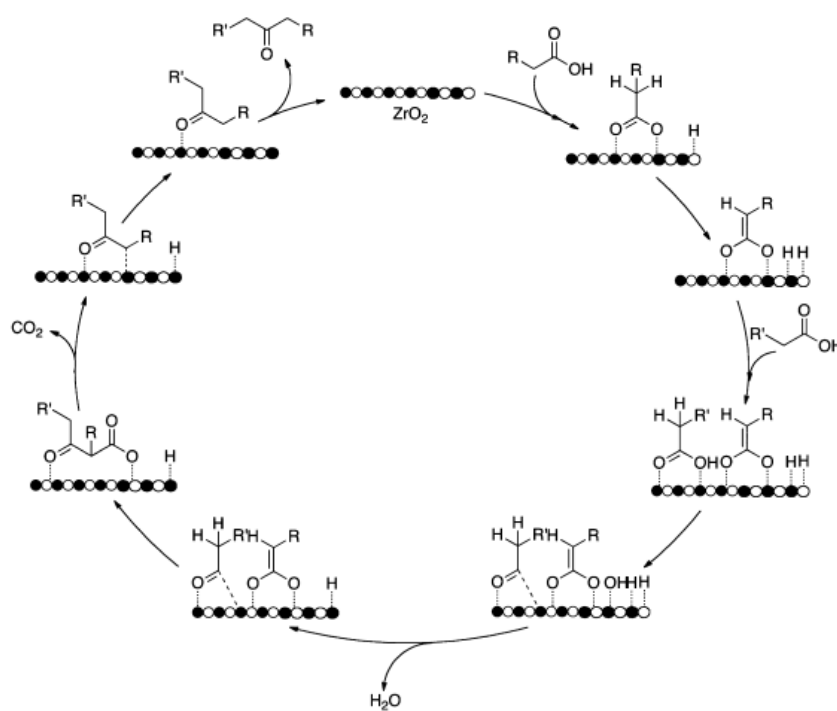


**Figure 2: Proposed mechanism for ketonization of carboxylic acid over ZrO<sub>2</sub> catalyst [35]**

However, most of these studies are on metal oxide catalyst and fewer studies on Brønsted acid catalysts exist.

Jacobs et al., studied the activity of acidic zeolites with different Si/Al ratios and discrete pore structures [34, 35]. They observed high selectivity of acetic acid reactions towards xylenol on H-ZSM5 at a temperature of 593K. With an increase in temperature, they observed an increase in selectivity to hydrocarbons. With their experiments with propionic acid they observed that the selectivity towards phenolics produced by aldol condensation of ketones decreased and the selectivity towards forming a ketone increased with butyric acid, the hypothesis being that the intermediates for forming phenolics are bulky and thereby not selective on H-ZSM5 zeolite.

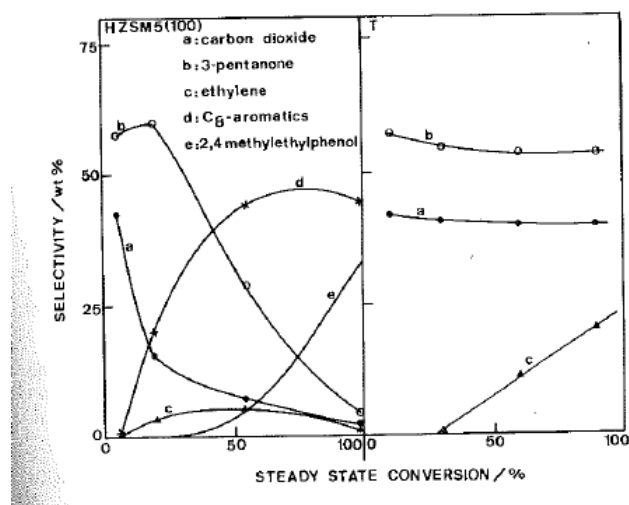
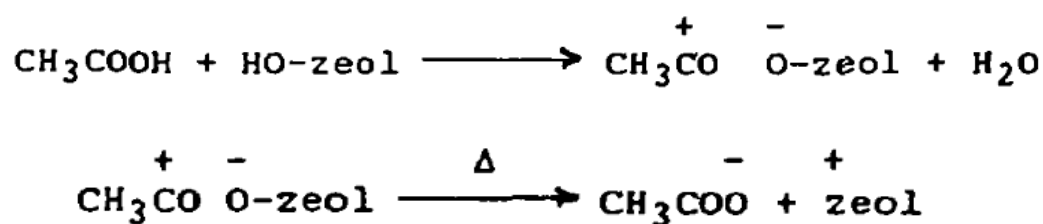


Figure 3: selectivity of propionic acid reactions in HZSM5 and HT zeolites[34]

Chang et al., from their studies proposed that the mechanism of ketonization occurs with the nucleophilic attack of an acyl ion, by an acetate species with CO<sub>2</sub> elimination[36]. They claim that unlike in oxides where the precursor for the acylium ion is a ketene intermediate, in zeolites the acylium ion is formed by dehydroxylating the zeolite surface. The acetate ion is resulted in at higher temperatures and they

concluded that the acyl is the precursor for acetate species and that the zeolite surface is regenerable after coke removal, thereby providing evidence against their claim that formation of acetate species destroys the crystallinity. They also performed experiments to observe that addition of methanol to the reaction can directly result in reaction with the acyl ion to form a ketocarbenium ion which is further converted into a ketone.



**Figure 4: Proposed ketonization mechanism of acetic acid on HZSM-5 by Chang et al showing dehydroxylation of zeolite [36]**

Jacobs et al., proposed that the ketonization reaction on acidic zeolites starts with the formation of an acyl ion, subsequent formation of an anhydride [34, 35]. With their earlier work with butyric acid on HT zeolite, they have reported that anhydride is one of the observed products. It has been established that acetic anhydride is used in Friedel-Crafts acylation reactions as it decomposes to form an acyl and carboxylic acid on H-ZSM5.

Acylation studies of Toluene and p xylene using carboxylic acid as acylating agent on Y type zeolites indicated that the % yield of acylated product increased with increased carbon chain length in the carboxylic acid used for acylation [37]. This might suggest that with increasing carbon chain length in the acid, the acyl stability may increase.

Stockenhuber et al., performed TPD experiments of acetic anhydride on Na and H forms of Beta zeolite to observe acetic acid and ketene desorption and studied acylation of anisole. In this work they proposed that ketene might be an effective acylation agent and that the mechanism of acylation proceeds through a ketene[38]. In a later work using isotopic labelling and  $^1\text{H}$  and  $^{13}\text{C}$  NMR studies they proposed a reaction pathway for the acylation reaction of anisole and acetic anhydride to p- methoxyacetophenone proceeds through an acyl and not a ketene [39]. The acyl intermediate formation may be the initial step of the ketonization reaction mechanism, but there are no studies yet to ascertain the specific details of the mechanism.

### **1.3. Previous work in our group[40]**

Several studies have been under progress in our group for identifying the reaction conditions for higher selectivity towards ketone, and for understanding mechanism of ketonization of acetic acid on the surface of zeolite catalyst.

Figure 5 shows the results from a Temperature Programmed Desorption (TPD) experiment with acetic acid over H-ZSM5, a clear initial dehydration step was reported and it was proposed that dehydration is a precursor to the formation of a surface acylium cation type intermediate, which further interacts with a second carboxylic acid

in the form of a tautomer and decomposes to form a ketone and CO<sub>2</sub>. Sufficient evidence and understanding about the tautomer species has to be obtained.

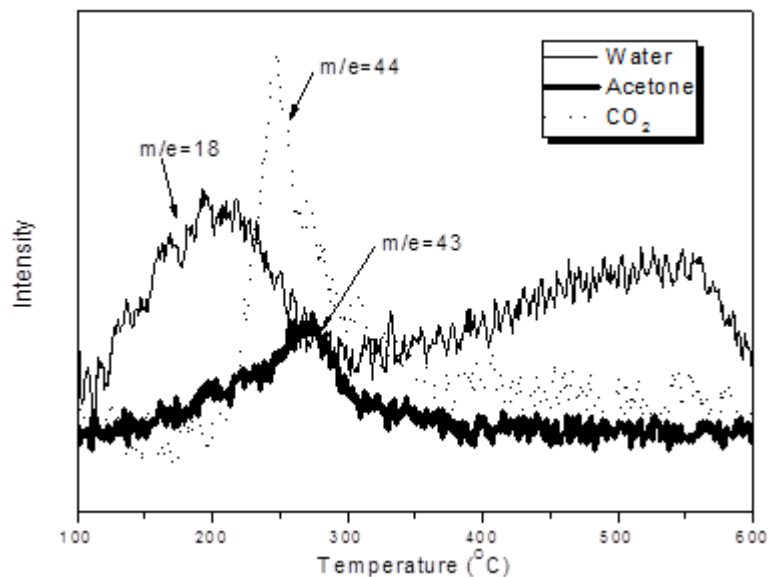


**Figure 5: Acetic acid TPD on HZSM-5 showing an initial dehydration step involved in the reaction pathway[40]**

Chang et al., proposed that the mechanism of ketonization on acidic zeolites can be assumed similar to that on titania catalyst and from acylium precursor, the acetate species formed dehydroxylates the zeolite surface [36].

From FTIR experiments our group provided evidence that after desorption of a ketone, the Brønsted acid sites on the zeolite surface are regenerated. These studies indicated that the reaction mechanism of ketonization over zeolites in does not dehydroxylate the surface.

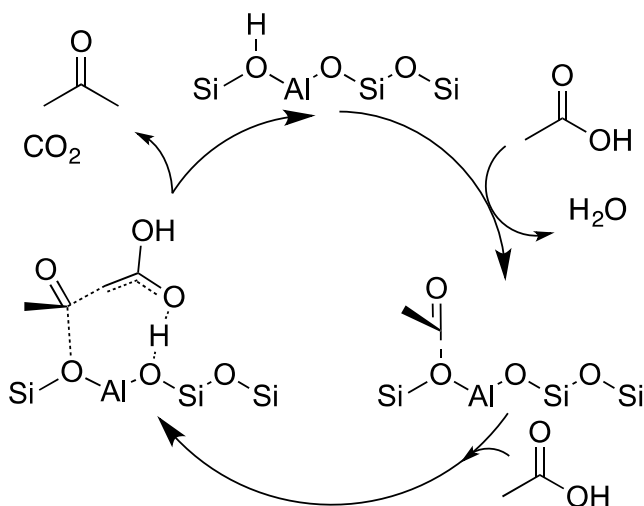


**Figure 6 : Proposed mechanism of ketonization over zeolites [40]**

The speculated mechanism from studies in our research group is that one carboxylic acid interacts with proton on the zeolite surface and dehydrates resulting in a surface acyl species as shown in figure 6. This acyl species couples with a second carboxylic acid in the form of an enolate species to result in a ketone. Studies are in progress to further understand the second carboxylic acid activation.

#### **1.4. Research Objectives**

With extensive research in our group, it has been established that over zeolite, a carboxylic acid dehydrates to form a surface acyl species, which couples with a second acid molecule to form an intermediate that decarboxylates to form ketone and CO<sub>2</sub>[40]. Following that study, my work focused on understanding the role of alpha hydrogen in the ketonization mechanism on zeolites which involves work with longer carbon chain

carboxylic acids, comparing activity of catalyst with pore sizes to understand the confinement effects on the ketonization reaction.

Performing gas phase flow experiments with various carboxylic acids with varying carbon chain length and number of alpha hydrogens like Pivalic acid, benzoic acid, propionic acid, hexanoic acid and  $^{13}\text{C}$  experiments will further improve our understanding the ketonization mechanism and the role of alpha hydrogen. Temperature programmed experiments with carbon labeled carboxylic acid can give an insight to the necessity of the presence of an alpha hydrogen for formation of surface acyls.

Diffusion limitations may play an important role in reactions involving longer or bulky acids. Zeolites with shorter diffusion paths lead to better activity of the zeolite for ketonization reaction of carboxylic acids.

Comparing the activity of different pore sized zeolites may play an important role in providing a better understanding of the ketonization on zeolites

## **2. Chapter 2: Experimental set up**

### **2.1. Catalyst Preparation**

The commercially obtained ammonium form of the ZSM5 catalyst was calcined in dry air at 600°C for 5 hrs. to thermally decompose  $\text{NH}_4^+$  to  $\text{NH}_3$  and  $\text{H}^+$  and obtain the protonated form of the zeolite. This catalyst sample will be hereby referred as H-ZSM5. This H-ZSM5 catalyst has a Si/Al ratio of 40.

The HY zeolite was purchased commercially in the hydrogen form with two Si/Al ratios 2.6 and 40. These two samples will be referred as HY2.6 and HY40 in this study.

The Beta zeolite with a Si/Al ratio of 19 purchased in the ammonium form was calcined at 600°C for 5 hrs to obtain the proton form of zeolite, this will be referred to hereby in this study as HBeta19.

The mesoporous catalysts used in this study were prepared in our laboratory using procedures from the literature as described in sections 3.5.1, 3.5.2 and 3.5.3.

The catalysts in their proton form, were pelletized and subsequently crushed and sieved to particles with size ranging from 90-250  $\mu\text{m}$ .

### **2.2. Flow reactor and conditions**

The continuous flow reactions were conducted in vapour phase at atmospheric pressure in a ¼"OD quartz reactor and at various temperatures ranging between 220 °C and 320 °C. The catalyst was mixed with acid washed glass beads of size ranging between 150  $\mu\text{m}$  – 250  $\mu\text{m}$  to avoid channelling and this was packed into a bed into the reactor held



between quartz wool plugs. A thermocouple was attached to the outer side wall of the reactor to monitor the temperature of the catalyst bed. A vaporization zone is created at the inlet of the reactor by heating it to appropriate temperatures sufficient to vaporize the reactants. The outlet lines are heated to a temperature of 250°C to prevent any condensation in the lines and the outlet of the reactor is connected to a six port valve and to a HP GC equipped with a flame ionization detector and an innowax column with dimensions 30m and 0.25  $\mu\text{m}$  for product analysis.

The acid reactants, Pivalic acid (Aldrich, 99% ), benzoic acid (Sigma Aldrich, ACS reagent,  $\geq 99.5\%$ ), acetic acid (Sigma Aldrich, ACS reagent,  $\geq 99.7\%$ ), propionic acid (Sigma Aldrich, ACS reagent,  $\geq 99.5\%$ ) hexanoic acid (Sigma Aldrich, ACS reagent,  $\geq 99.5\%$ ), Furoic acid (Aldrich, 98%), succinic acid (Sigma Aldrich, ACS reagent,  $\geq 99.0\%$ ), Methyl acetate (Aldrich  $\geq 98\%$ ), ethyl acetate (Aldrich, 99.8%), were introduced into the reactor with a syringe pump. The products made in the reaction were condensed into a sample bubbler using ice as a cooling medium, at the downstream of the six port valve. The collected products were analysed in a mass spectrometer. The reactions were conducted at various temperatures and Weight/ flow (W/F) ratios.

## **2.3. TPD experiments – set up and conditions**

### **2.3.1. IPA - TPD experiment setup**

IPA (Isopropyl Amine) Temperature - programmed desorption (TPD) experiments was performed on the H-ZSM5 sample and the mesoporous catalysts to quantify the number

of Brønsted acid sites in the catalyst sample. 50mg of the catalyst sample was held between quartz wool plugs in a ¼"OD quartz reactor. This sample was pretreated at 300 °C with 20ml/min helium flowing as carrier gas for 2 hours. The temperature was then reduced to 100°C and IPA was injected into the reactor as 2 µL pulses until saturation. An MKS cirrus 200 mass spectrometer was used to track the m/e (mass to charge ratio) of IPA 44 and 58 for a constant signal indicating saturation. The catalyst bed was flushed with a helium flow of 20ml/min for 4 hours to ensure that the bed was free of any physically adsorbed IPA. The temperature of the catalyst bed was ramped from 100 °C to 600 °C at a rate of 10°C/min and the products desorbing from the surface are tracked in the mass spectrometer. Propylene gas was pulsed from a known volume sample loop to quantify the products.

### **2.3.2. TPD experiment setup**

TPD experiments were performed in my study to understand the mechanism of the ketonization reaction of different acid and analyze the results. These experiments were performed in a quartz tube reactor of size ¼"OD. The outer wall of a reactor is attached with a thermocouple near to the catalyst bed, which is used to control the temperature inside the furnace. After pretreatment of the catalyst, the carboxylic acid is pulsed into the reactor in small amounts (1 or 2µL pulses) using a 10µL syringe so that the acid sites in the catalyst bed are saturated. The MKS cirrus 200 mass spectrometer was used to track the corresponding masses of the reactants pulsed in to ensure constant signal peak area indicating saturation. The catalyst bed was flushed for 4 hours in helium flow

(50ml/min) to remove any physically adsorbed species. After flushing to remove physically adsorbed species on the catalyst surface, the temperature is ramped from 100°C to 600°C at a rate of 10 °C/min. The mass spectrometer was used to track the m/e (mass to charge ratio) of the expected products and analyzed for further understanding.

### **2.3.3. Pulsing experiments with two acids and TPD**

The experiment setup of the quartz reactor, the mass spectrometer and the pretreatment conditions are as described in section 2.2.2. The catalyst bed is saturated with one of the acids pulsed in with a 10µL syringe. After flushing for few hours, the temperature is ramped at a rate of 10 °C/min to a pre-identified dehydration temperature (depending on the experiment being performed) and the second carboxylic acid is pulsed in with a 10µL syringe. The outlet stream of the reactor is analyzed using a MKS Cirrus MS. The idea behind these experiments was to saturate the zeolite surface with one acid molecule, dehydrate and supply the surface with a second acid molecule to analyze the products formed.

### **2.4. BET experiments – Set up and experiment**

To determine the total pore volume, micropore volume of the catalyst samples, a Micrometrics ASAP 2020 Surface Area and Porosity Analyzer (Micrometrics; Norcross, GA) was used to perform nitrogen adsorption experiments. The difference between total pore and the micropore volume also gives the mesopore volume of the catalysts.

The catalyst sample was degassed at 250°C for 12 hours before performing the adsorption experiment.

## **2.5. XRD experimental setup**

X-Ray Diffraction studies were performed on the zeolite sample for checking the crystallinity of the zeolite. The catalyst sample was put on a plastic slide, with the surface made very flat. The analysis was performed using Rigaku automatic diffractor (model D-Max A) with a curved crystal monochromator. It was operated at 40 kV and 35mA between the angle ranges of 5- 55° using Cu K $\alpha$  as radiation source.

## **2.6. SEM experimental set up**

To estimate the particle diameter of the samples, SEM (Scanning electron microscopy) measurement of the sample was performed using a Zeiss- NEON FEG-SEM instrument. A small amount of the zeolite was suspended in aqueous medium and placed on carbon tape and dried before analyzing.

### 3. Chapter 3 : Results and Discussion

#### 3.1. Pivalic acid

Ponec et al.,[20] conducted experiments with different acids varying number of alpha hydrogens and their results show that with decrease in number of alpha hydrogens, the ketone formation decreased. Pivalic acid, isobutyric acid, propionic acid and acetic acid were used for this study and the results are shown in figure 7.

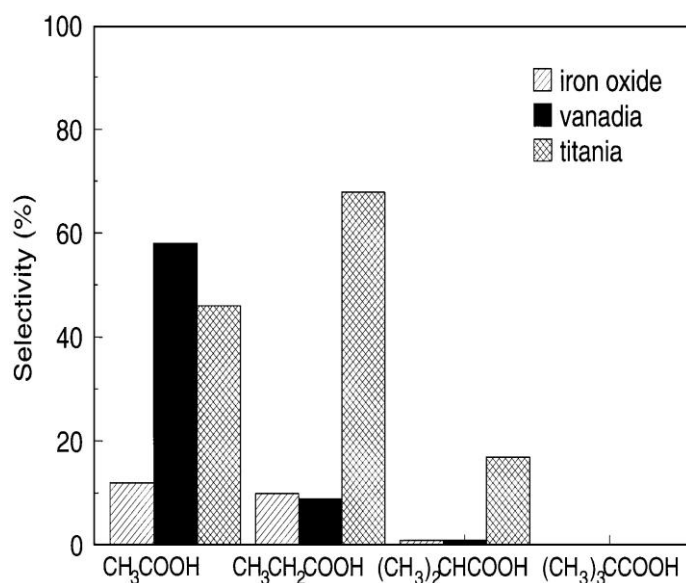


**Figure 7: Graph showing selectivity towards ketone formation in reaction of 4 acids with decreasing number of alpha hydrogens on three different oxide catalysts[20]**

To understand the mechanism behind the ketonization reaction, Ponec et al., [20] conducted carbon labelled experiments. Figure 8 shows their results based on which they concluded that a reaction intermediate is not a ketene as few studies speculate, but a species similar to ketene.

Occurrence of the Labeled and Unlabeled Forms of Some Products in the Reaction over Titania		
Reactants	Products	
	Labeled	Unlabeled
$\text{CH}_3\text{-}^*\text{C}(=\text{O})\text{OH}$	$\text{CH}_3\text{-}^*\text{C}(=\text{O})\text{-CH}_3$ 100%	$\text{CH}_3\text{-C}(=\text{O})\text{-CH}_3$ 0%
$\text{CH}_3\text{-}^*\text{C}(=\text{O})\text{OH}$ $\text{CH}_3\text{-C}(\text{CH}_3)_2\text{-C}(=\text{O})\text{OH}$	$\text{CH}_3\text{-C}(\text{CH}_3)_2\text{-}^*\text{C}(=\text{O})\text{-CH}_3$ 0%	$\text{CH}_3\text{-C}(\text{CH}_3)_2\text{-C}(=\text{O})\text{-CH}_3$ 100%

**Figure 8: Experimental results with labelled acetic acid and Pivalic acid reactions over Titania reported in literature [20]**

The aim of our research was to determine if a similar mechanism occurs over zeolites and if the alpha hydrogen is important for reaction over zeolites. Pivalic acid which has no alpha hydrogen was selected to probe this reaction over zeolites. Pivalic acid is a crystalline solid, it was made into a solution in a molar ratio of solute to solvent 10:1 with benzene as a solvent. This solution will be referred as pivalic acid in further discussion. Flow reactions with Pivalic acid over H-ZSM5 at a reaction temperature of 300 °C and a W/F of 0.12 show 100% selectivity towards isobutylene.

To ensure that there are no solvent effects hindering product formation, experiments were performed varying the solvent to solute ratios to benzene and Pivalic acid. For these experiments the catalyst weight was maintained constant and the reaction temperature was at 220°C, the selectivity towards isobutylene remained constant with

different solutions varying the solute solvent ratio. Solute solvent ratios of 10:1, 1: 10 and 1: 30 were experimented with to show 100% selectivity towards isobutylene.

The possibility of change in selectivity with varying temperatures was examined by conducting reactions over varying reaction temperatures over a range of 220°C to 300°C with a W/F of 0.041. The conversion of the Pivalic acid slightly changed at various temperatures, but the selectivity remained 100% towards isobutylene, thereby indicating the fast decomposition of the Pivalic acid and no ketonization. Figure 9 illustrates these results, the carbon balance remained above 90% for these experiments.

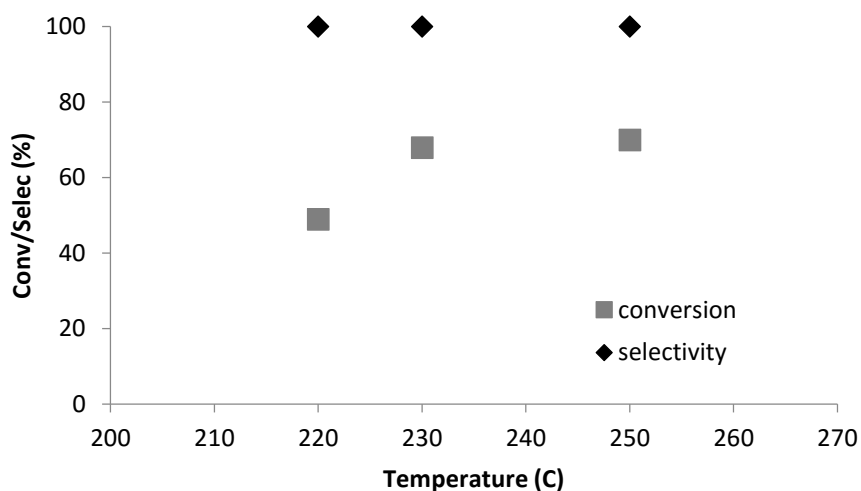


**Figure 9: Flow reaction studies with Pivalic acid showing conversion and selectivity with varying reaction temperatures at constant W/F = 0.041**

To investigate the probability of cross ketonization, co-feeding experiments with pivalic acid and acetic acid in a molar ratio of 5:1 were conducted at reaction temperature of 300 °C and a W/F of 0.3 with respect to acetic acid. The products formed were acetone

and isobutylene, and no cross ketone was formed between both acids, but the interesting observation here was the reduced activity of acetic acid ketonization on H-ZSM5 when co-fed with pivalic acid. To look for competitive adsorption between pivalic acid and acetic acid on the zeolite surface, an experiment was performed where both acids were fed into the reactor and pivalic acid stopped midway of the reaction. Figure 10 shows the amounts of acetone produced by reacting acetic acid alone over HZSM -5 at 300°C and W/F =0.3 and the amount of acetone formed when both acids were co-fed. Comparing the amounts of acetone produced, it can be noticed that the activity of acetic acid when co-fed with pivalic acid is significantly low. But, when the flow of pivalic acid was stopped, it can be observed that the amount of acetone produced increased and is comparable to acetone produced when acetic acid is fed alone. Re-starting the pivalic acid flow, inhibits the amounts of acetone produced. This suggests that the pivalic acid only competes for the sites on the surface but does not adsorb irreversibly on Brønsted acid sites.



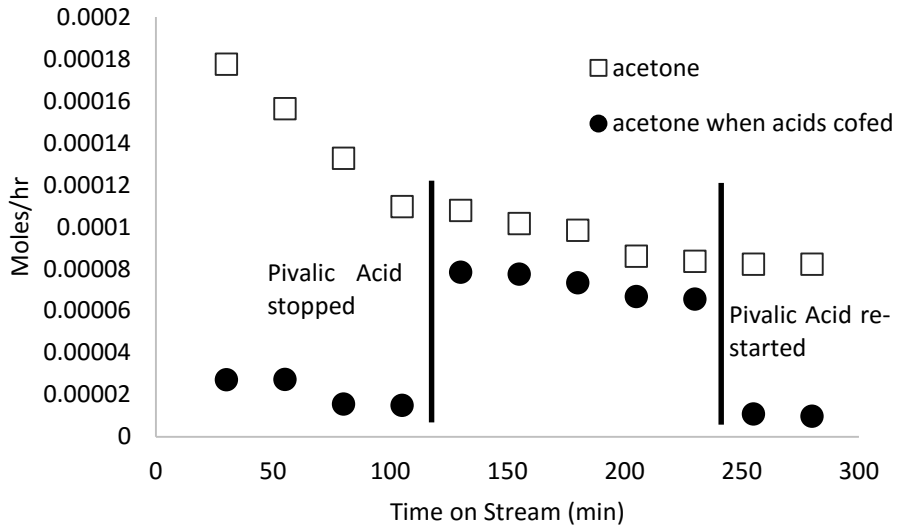


**Figure 10: Flow reaction comparison between acetic acid ketonization vs ketonization of acetic acid when co-fed with Pivalic acid (molar ratio = 1: 5) at T=300°C and W/F =0.3 w.r.t. acetic acid**

Previous studies in our group have reported the acetic acid ketonization mechanism over HZSM-5 catalyst, where an initial dehydration step resulting in the formation of acyl intermediate as reported in section 1.3. The reaction mechanism was proposed to be the interaction of the surface acyl intermediate with a second activated surface acid species followed by decomposition of the intermediate into acetone and CO<sub>2</sub>[40].

Temperature Programmed Desorption studies can indicate if there an initial dehydration of the acid on the surface of the catalyst. TPD experiments with pivalic acid were performed on H-ZSM5 catalyst and masses for water (m/e =18), CO (m/e = 28), CO<sub>2</sub> (m/e = 44), Pivalic acid (m/e = 57) and isobutylene (m/e = 41) were tracked, shown in Figure 11. The graph implies that the pivalic acid does not dehydrate to form a stable

surface acyl, instead it decomposes. These observations are in line with the flow reaction results from which we observe that pivalic acid does not undergo ketonization.

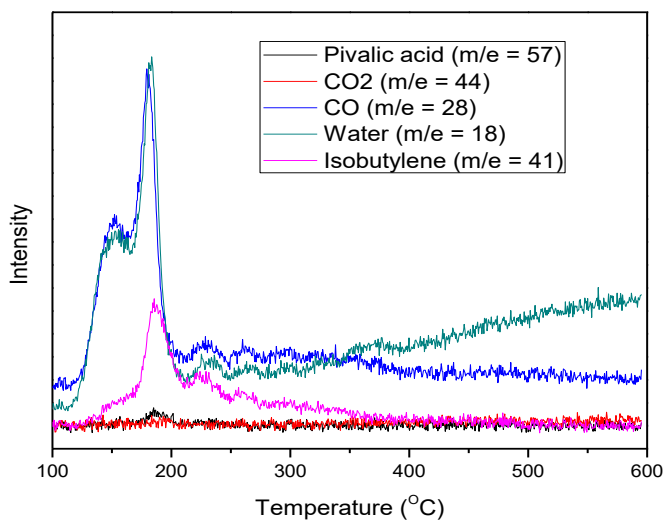


**Figure 11: Pivalic acid TPD on H-ZSM5 showing decomposition into isobutylene, water and CO<sub>2</sub>**

Mark Davis et al.,[41] observed during acylation of biphenyl with pivalic acid, that the acyl formed from a pivalic acid is very unstable compared to the isobutyl cation that is formed due to its decomposition and therefore their expected product could not be achieved from the acylation reaction at the reported conditions. Our results are in line with these observations indicating pivalic acid decomposes very fast.

### **3.2. Benzoic acid and <sup>13</sup>C labelled benzoic acid**

Experiments for ketonization with carboxylic acids having no alpha hydrogens and <sup>13</sup>C labelled acids gave interesting perceptions into the importance of the alpha hydrogen importance for forming a ketone. As discussed in the section 3.1 figure 7 , the result

from Ponec et al., experiment of showing reducing ketone formation with a decrease in number of alpha hydrogens was attributed to steric hindrance or the necessity of an alpha hydrogen[20]. To understand what plays the role in reduced ketone production, they conducted experiments with benzoic acid, a molecule with no alpha hydrogen and less steric hindrance. Their experiments with benzoic acid showed that the acid does not form a ketone. Benzoic acid is not a sterically hindered molecule but the alpha hydrogen is absent. They concluded that an alpha hydrogen is important and maybe involved in the reaction but no further evidence has been provided to see how the alpha hydrogen participates in the mechanism[20].

In this work we wanted to understand if benzoic acid can form a ketone over zeolites and subsequently how the alpha hydrogen can affect the selectivity towards forming ketones. To study this, various experiments have been performed using benzoic acid, acetic acid and  $^{13}\text{C}$  labelled benzoic acid.

Benzoic acid is a crystalline substance, it was made in to a solution with benzene as a solvent. This solution of molar ratios of benzoic acid to benzene of 1: 10 will be hereby referred as benzoic acid. Flow reaction results with benzoic acid on HZSM-5 at 300°C, a W/F of 0.22 and atmospheric pressure show zero conversion with time on stream. Various reaction temperatures were experimented with, but benzoic acid displayed no conversion into ketones or any other products.

As discussed in section 1.3, studies in our group have reported TPD experiments results, showing an initial dehydration step resulting in the formation of acyl intermediate was observed followed by a ketone and CO<sub>2</sub> [40].

Temperature programmed desorption (TPD) studies would indicate if the benzoic acid molecule dehydrates or decomposes. Benzoic acid TPD study shows the desorbing species with a temperature ramp, after benzoic acid is adsorbed on the catalyst surface, shown in Figure 12. It indicates an initial dehydration step suggesting the production of surface acyl species on the catalyst surface, but as expected, no self-ketone of benzoic acid was observed.

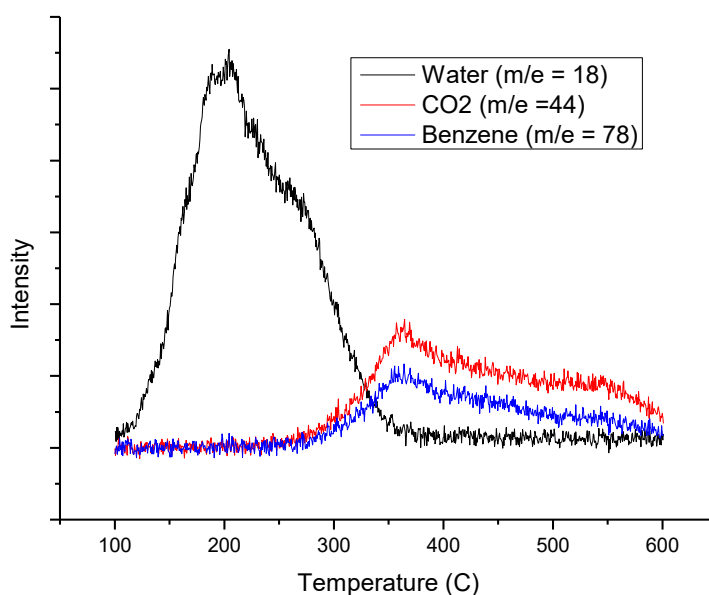


**Figure 12 : Benzoic acid TPD on H-ZSM5 showing an initial dehydration step involved in the mechanism**

It is expected to observe benzene and CO desorbing resulting from the surface adsorbed benzoyl species decomposition at higher temperatures. A small peak of CO ( $m/e = 28$ ) was observed with a high baseline. We believe that the  $\text{CO}_2$  observed is from the decomposition of physically adsorbed benzoic acid.

To ensure that the water desorbed is produced by the reaction of the benzoic acid on the Brønsted acid sites, the water formed on the catalyst surface was quantified corresponding to the available Brønsted acid sites in the catalyst sample. The number of moles of water desorbed was quantified to be 20.7 micromoles, and the number of Brønsted acid sites in the catalyst sample is 20.3 micromoles. The water generated corresponds to nearly 100% of the Brønsted acid sites, indicating that water is produced by reaction on the acid sites and is not physically adsorbed water. So it can be clearly assumed that the benzoic acid forms surface acyl species. Co-feeding of benzoic acid with another acid that can couple with the acyl from benzoic may provide us some insight into the ketonization reaction.

### **3.2.1. Co-feeding acetic acid and Benzoic acid**

Chang et al [36], in their studies proposed that the mechanism of ketonization occurs with the nucleophilic attack of an acyl ion, by an acetate species with  $\text{CO}_2$  elimination. Work by Ponec et al [19, 20, 30] about ketonization on various oxides with different acid reactants indicates that the presence of alpha hydrogen is important for ketonization over oxide catalysts. But 2,2,5,5, tetra methyl adipic acid, which lacks an alpha hydrogen forms a ketone over BaO and K.[31]. However, no discussion about the necessity of an

alpha hydrogen for ketonization over zeolites was available in literature. It may be noted that benzoic acid has no alpha hydrogen and this may be the reason that ketonization of benzoic acid on zeolites is not observed.

To further understand the role of alpha hydrogen in ketonization, co-feeding experiments with benzoic acid and another carboxylic acid containing alpha hydrogens was the next step to examine. Acetic acid seemed to be the best choice as it has three alpha hydrogens and from previous work in the group, it was established that acetic acid readily forms acetone [40] at similar reaction conditions.

Flow experiments co-feeding Benzoic acid and acetic acid in a molar ratio of 1: 8 at a reaction temperature of 300°C and W/F of 0.22 were performed, and the results are shown in Figure 13. We see acetone formation but an observation of great interest here, is the formation of acetophenone, a cross ketone between benzoic acid and acetic acid, with good carbon balances.

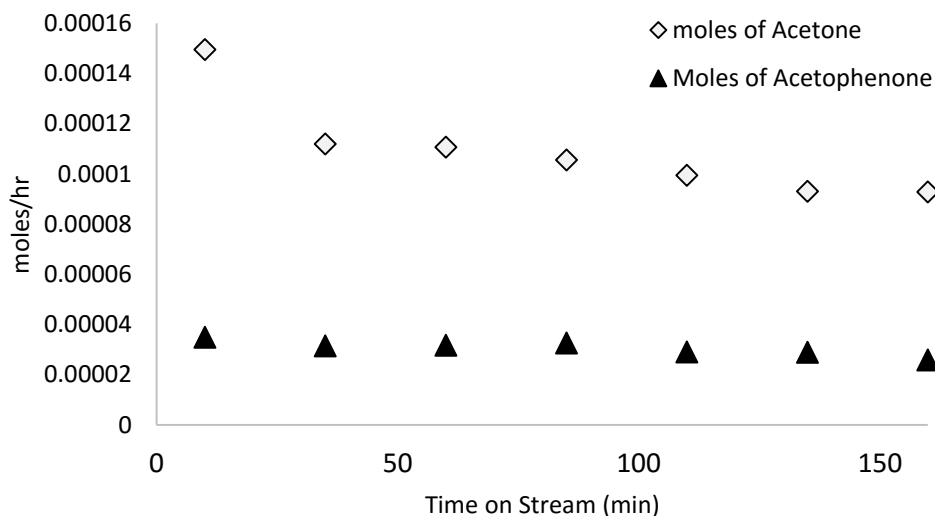


**Figure 13: Flow reaction studies co-feeding acetic acid with benzoic acid (molar ratio = 1:8) at T=300C and W/F =0.22, showing formation of two ketones**

Temperature programmed desorption studies were done for understanding the mechanism involved as described in section 2.3.3. From previous TPD experiments, the dehydration temperature is known just beyond which and the catalyst surface is believed to contain surface acyl species. The catalyst bed was saturated with benzoic acid, the temperature was ramped at 10 °C/min to 220 °C (pre-identified dehydration temperature of benzoic acid) and acetic acid was pulsed in through the septum on to the catalyst bed. The desorption of the ketones were tracked in the MS and are shown in Figure 16 a,b as a function of number of pulses.

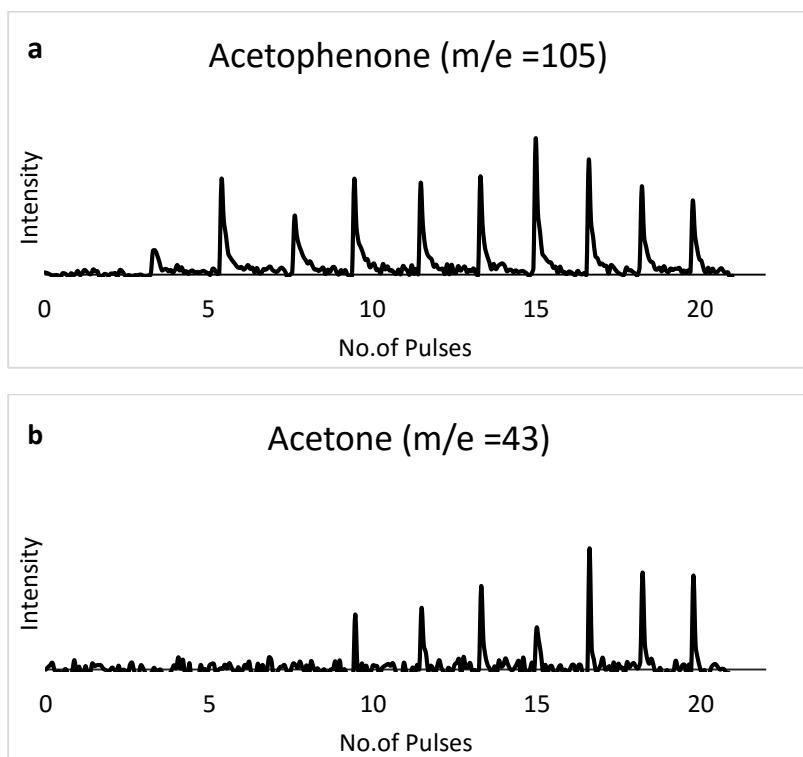


**Figure 14 a, b: Benzoic acid TPD studies pulsing in acetic acid on benzoyl adsorbed HZSM5 showing acetophenone and acetone respectively**

It was evident that a cross ketone is formed with acetic acid pulses. Also, an interesting observation is that with increase in number of pulses of acetic acid, the acetone peaks increases. This suggests that the surface adsorbed acyl species from benzoic acid interacts with the acetic acid molecules pulsed in to form acetophenone and desorb from the surface of the catalyst. With increased number of pulses, the surface benzoic-acyl species are reduced as they couple with acetic acid and leave the surface making the Brønsted acid sites available for acetic acid self-ketonization. Therefore, the acetone formation occurs after few pulses and seems to be more significant in the later pulses.

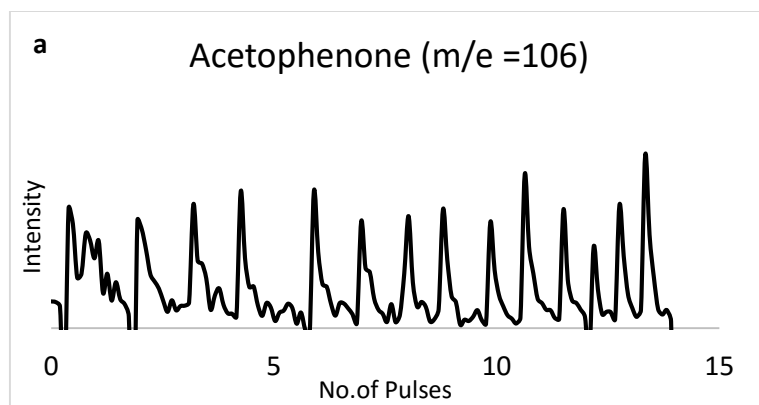


It can be established that for ketonization over zeolites, it is necessary that one of the two carboxylic acids has an alpha hydrogen.

### 3.2.2. Carbon Labelled experiments

From the experiments illustrated in the previous section, it was understood that one of the two acids reacting over HZSM-5 needs to have an alpha hydrogen to produce a ketone. But benzoic acid, which does not have an alpha hydrogen can produce surface acyl species was another result from the experiments. To support this observation, carbon labelled studies might help understanding the contribution from each acid for forming a ketone and thereby the reaction mechanism.

Temperature programmed experiments as described in section 2.3.3 were conducted with benzoic acid having  $^{13}\text{C}$  labelled carboxylic group and acetic acid. The catalyst surface was saturated with  $^{13}\text{C}$  labelled benzoic acid and the temperature was ramped to the dehydration temperature and acetic acid was pulsed in and the ketones were tracked for analysis and shown in Figure 15 a,b.



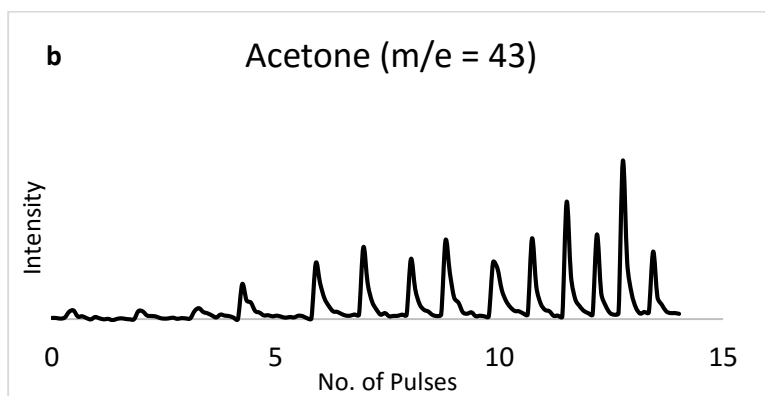


**Figure 15 a, b: Benzoic acid TPD studies pulsing in acetic acid on  $^{13}\text{C}$  labelled benzoyl adsorbed HZSM5 showing acetophenone and acetone respectively**

Figure 15a shows the spectrum for  $m/e = 106$ , where as the mass number that is corresponding to the acetophenone is  $m/e = 105$ . The observation of significance from this experiment is that, the mass number ( $m/e = 105$ ) for the cross ketone, acetophenone shifted by 1. This indicates that the cross ketone contains the  $^{13}\text{C}$  labelled carbon. This is strong evidence that the acyl species present in the cross ketone is contributed by the benzoic acid and not the acetic acid. The acyl from Benzoic acid couples with an activated species formed by acetic acid resulting in an intermediate subsequently decomposing into a ketone and  $\text{CO}_2$ .

From this study, we can conclude that atleast one alpha hydrogen is required in one the acids reacting to form a ketone over zeolites.

### 3.3. Propionic acid

Working with other acids containing alpha hydrogens may give us further insights about the reaction mechanism, the involvement of alpha hydrogen in forming the second species that couples with the acyl to form a ketone intermediate.

Propionic acid is a three carbon chain length carboxylic acid, which has two alpha hydrogens. From my previous work with benzoic acid, we could conclude that at least one acid should have an alpha hydrogen to form ketone. Therefore it can be expected that propionic acid can undergo a ketonization reaction to form a symmetrical five carbon ketone on H-ZSM5 catalyst.

To get a better insight on the probable mechanism for the ketonization reaction, cross coupling reaction possibility between propionic acid and acetic was to be studied.

Flow reactions with propionic acid co-fed with acetic acid in a molar ratio 1:1 were performed in the system described in section 2.1 over H-ZSM5 catalyst surface at a reaction temperature of 300°C with a W/F = 0.31 and atmospheric pressure. The products observed from flow reactions are a four carbon cross ketone between both acids, a symmetrical ketone from each acid are shown in figure 16. The observation of interest in this reaction is that the selectivity towards a cross ketone from this reaction is higher than that of the corresponding self- ketones.

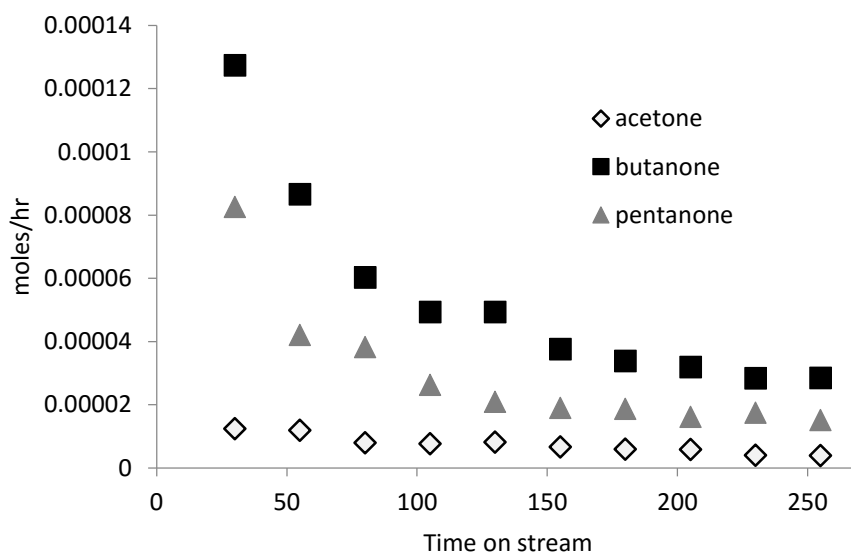


**Figure 16 : Flow reaction studies of propionic acid co fed with acetic acid in a molar ratio 1:1 and W/F = 0.3 w.r.t acetic acid at T=300C**

Figures 17 and 18 show the results from co-feeding reactions of propionic acid and acetic acid at a similar W/F as the previous reaction but at higher temperatures. The reaction was conducted at higher temperatures to understand if temperature played an effect on the selectivity towards the cross ketone. As we can see, the selectivity towards the cross ketone remains unaltered with temperature. The carbon balances in these flow reactions were good and remained above 90%.

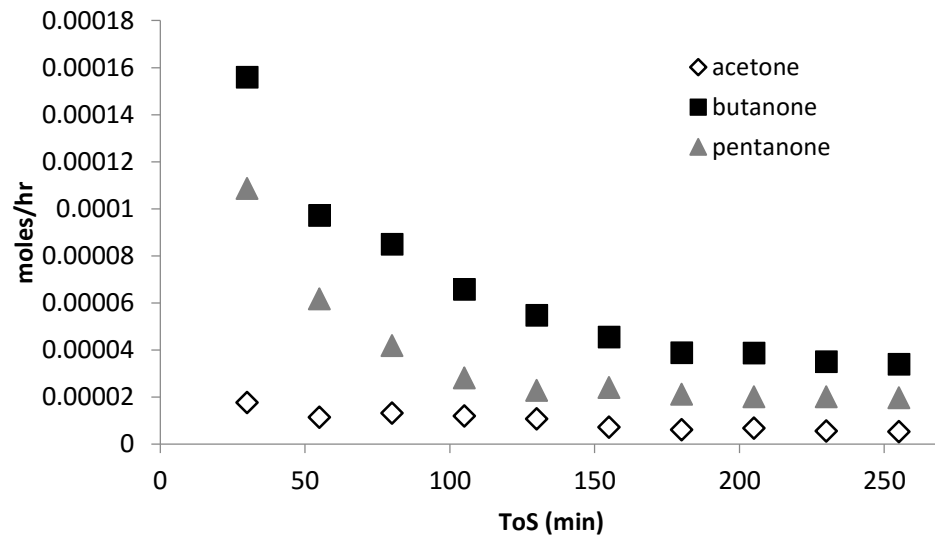


**Figure 17: Flow reaction studies of propionic acid co fed with acetic acid in a molar ratio 1:1 and W/F = 0.3 w.r.t acetic acid at T=315C**

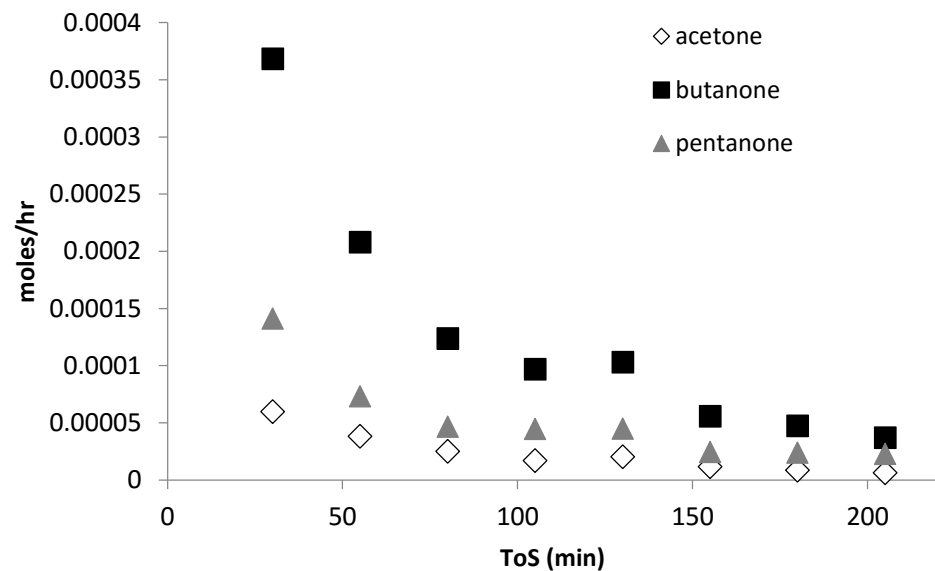


**Figure 18: Flow reaction studies of propionic acid co fed with acetic acid in a molar ratio 1:1 and W/F = 0.3 w.r.t acetic acid at T=325C**

To ensure that these reaction results are not limited by mass transport, we performed the experiments at different carrier gas velocity (50ml/min, 75 ml/min, 100ml/min and 125 ml/min) as it has been well established that at high gas velocity conditions external mass transfer limitations can be avoided[42]. The reactions were performed under the conditions with no mass transfer limitations at 100ml/min.

Temperature programmed desorption studies for propionic acid were performed to understand if the mechanism is any different from the other acids studied until now, figure 19 shows the results. The interesting observation here is that, although there is a clear dehydration step involved in the mechanism, we see a more significant peak of water (m/e=18) desorbing at a higher temperature.

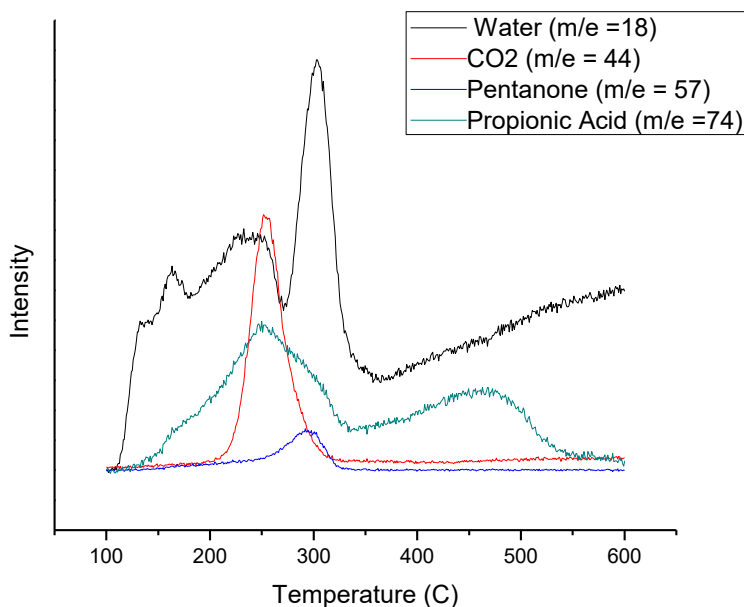


**Figure 19: TPD experiment of propionic acid showing dehydration on the catalyst surface with increasing temperature**

Also, other hydrocarbons appear in this TPD experiment as shown in the Figure 20. The spectrum for masses 39, 41, 42 show the desorption of propene, indicating that there might be aldol condensation happening on the surface.

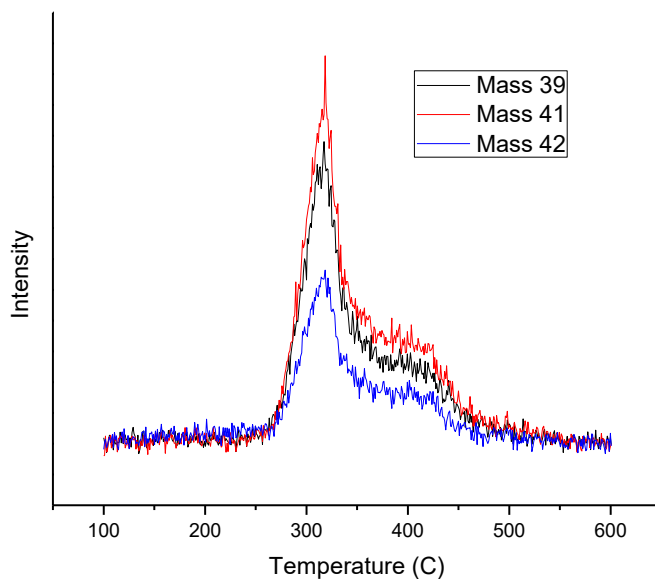


**Figure 20: TPD experiment of propionic acid showing desorbing hydrocarbons with increasing temperature**

To gather further evidence on the probable condensation occurring, TPD experiment was performed with 3-pentanone and the figures 21, 22 show the mass of water ( $m/e = 18$ ) and hydrocarbons (propene  $m/e = 39, 40, 41$ ) tracked during the temperature ramp up. As we can clearly see, a significant peak showing water is desorbing at a temperature of 300°C and the propene peaks are very similar to the ones we observed during the TPD experiment of propionic acid. Hence, we can confirm that the mechanism involves

initial dehydration step resulting in acyl formation but the later peak of water is from aldol condensation of the ketone.

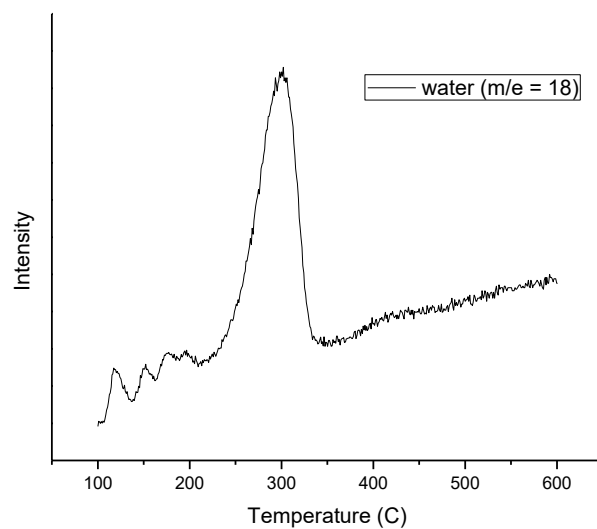


**Figure 21: TPD experiment of Pentanone showing water desorbing at higher temperature confirming aldol condensation during propionic acid TPD**



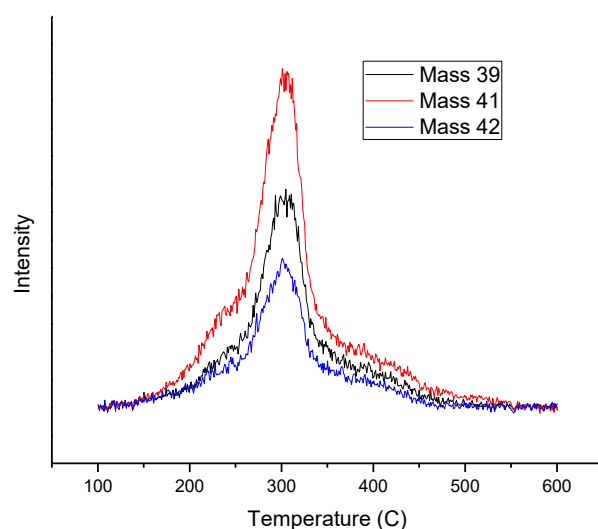


**Figure 22: TPD experiment of Pentanone showing hydrocarbons confirming aldol condensation during propionic acid TPD**

Therefore, we can confirm that the ketone produced in this reaction undergoes aldol condensation and results in alkanes, alkenes and other fragmented hydrocarbon products. This makes the reaction complicated to further study and understand the mechanism using TPD studies. So from the propionic acid studies showing higher cross ketone selectivity, we could hypothesize that the reason for higher cross ketone selectivity can be the ease of formation or the stability of the acyl species increases with increased carbon chain length.

### **3.4. Hexanoic acid**

From the studies with propionic acid we could see that the primary product for co-feeding reactions with acetic acid and propionic acid is a cross ketone between the two

acids. This is unlike studies reported in the literature. Understanding if the acyl formation and acyl stability increases with carbon chain length would help understand the mechanism of ketonization over zeolites better.

Hexanoic acid was co fed along with acetic acid into the flow reactor to observe if the selectivity towards the cross ketone is still high as shown in figure 23. At very low partial pressures of hexanoic acid (molar ratio of 1: 10 of hexanoic acid and acetic acid), It is observed the cross ketone is the highly selective product, but the conversions are low compared to the shorter carbon chain acid conversion. There is a possibility as the H-ZSM5 pores are small for desorption of the bulky products formed as we expect an eleven carbon chain symmetrical ketone from hexanoic acid and a seven carbon chain cross ketone.

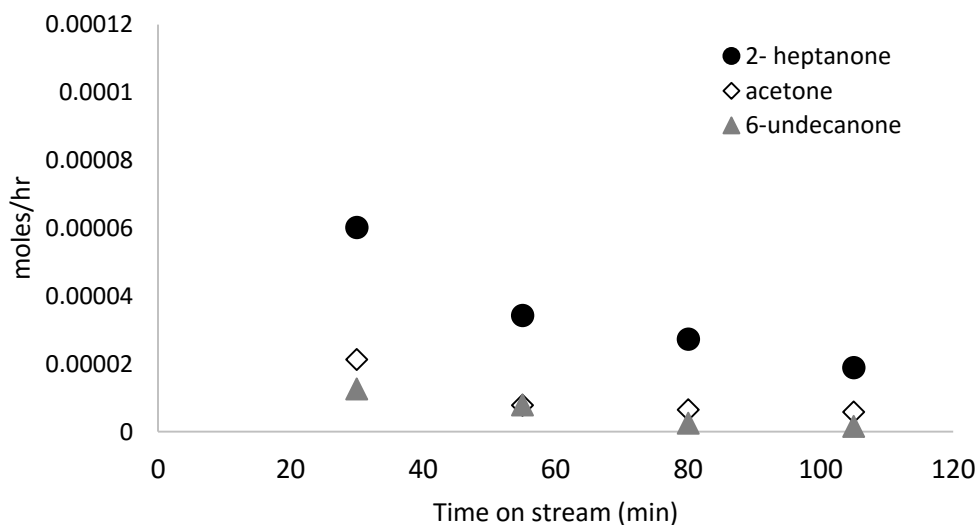


**Figure 23: Flow reaction studies of hexanoic acid co fed with acetic acid at T=300C over HZSM-5 showing cross ketone as a primary product with very low partial pressures of hexanoic acid**

### 3.4.1. Different catalysts

The very low conversions of this reaction led us to examine the activity of larger pore zeolites like H-Y and H-Beta. The same reaction was conducted at similar conditions with HY zeolite of Si/Al ratio of 2.6 and 40, and H-Beta zeolite of Si/Al ratio of 19.

For comparison between all the catalyst samples, the TOF (turn-over frequency) for the cross ketone formed on each Brønsted acid site is plotted as a function of time on stream and shown in figure24. Surprisingly, the HY and H-Beta did not show similar activity for the formation of ketones in this reaction.

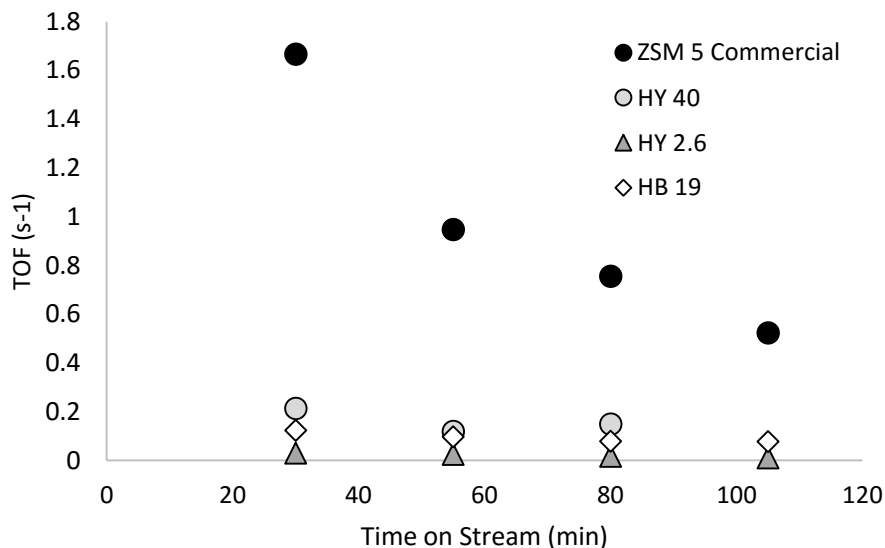


**Figure 24: Flow reaction results of hexanoic acid co fed with acetic acid (molar ratio = 1 : 10) at T=300C over HZSM-5, H-Beta and HY showing TOF for cross ketone**

Figure 25 shows the TOF compared for the different catalysts for the activity towards the self- ketone formation. As it can be seen that H-ZSM5 deactivates rapidly as compared to HY-40, but the deactivation can be due to higher conversion on H-ZSM5,

and blocking of the catalyst pores from un-desorbed products. However, the activity is lower in the other zeolites compared with H-ZSM5.

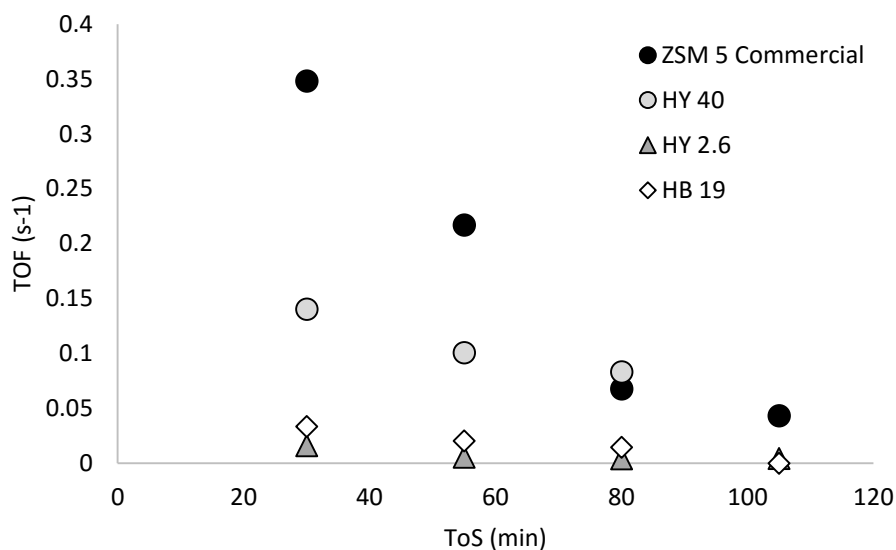


**Figure 25: Flow reaction results of hexanoic acid co fed with acetic acid at T=300C over HZSM-5, H-Beta and HY showing TOF for self-ketone of Hexanoic acid**

To continue studying the hexanoic acid activity over H-ZSM5 catalyst, the idea of creating mesopores in the MFI framework zeolite to shorten the diffusion path for the reactants and products seemed an interesting route to explore.

### 3.5. Mesoporous catalyst

Increasing the activity of a zeolite is proposed to be achieved by shortening the diffusion path for the reactants to reach an active site in the pores or for desorption of a formed product. This can be done by varying the crystallite size or creating mesopores into the zeolite framework [43-47]. With decrease in the diffusion path length in the catalyst, the activity is expected to increase towards longer chain products. It was believed that a

shorter diffusion path might be able to increase the activity of the catalyst for hexanoic acid ketonization.

### **3.5.1. Preparation of Parent zeolite**

ZSM-5 catalyst was synthesized hydrothermally following the procedure specified in literature by Armaroli et al[44]. The reagents used for the synthesis are Tetraethyl orthosilicate (98%, Sigma Aldrich), tetrapropylammonium hydroxide (40% W/W, Alfa-Aesar), aluminum isopropoxide (98%, Sigma-Aldrich), sodium hydroxide (>98%, Sigma-Aldrich) and double distilled water. The sample was washed thrice with double distilled water and filtered by centrifugation. The sample was subsequently dried overnight for around 12 hours in an oven at 85°C. Ion- exchange procedure was carried out with the sodium form dried sample to ammonia with a 2M ammonium nitrate solution at 80°C for 3 hours. To ensure complete exchange, this procedure was repeated 5 times, followed by washing the sample thrice with double distilled water and overnight drying at 85°C. This ammonium form of the zeolite was calcined at 600°C, ramp rate at 2 °C/min for 5 hours to get proton form of zeolite by thermally decomposing  $\text{NH}_4^+$  to  $\text{NH}_3$  and  $\text{H}^+$ . This H-ZSM5 sample will be hereby referred as the Parent zeolite. The parent zeolite was used to create a mesoporous zeolite using de-silication approach as described in section 3.5.2, this sample will be referred as Mesoporous zeolite. This mesopore was acid washed as described in section 3.5.3, the acid washed sample will be referred as acid washed mesopore in further discussion. SEM was performed on these catalyst series from which crystal sizes are obtained tabulated in table 1.

<b>Sample</b>	<b>Crystal size (SEM, <math>\mu\text{m}</math>)</b>
Parent zeolite	10
Mesoporous zeolite	10
Acid-washed Mesopore	10

**Table 1: Synthesized Mesopore series characterization SEM results for crystal size**

### **3.5.2. De-silication to produce mesopores**

It is reported in literature that alkaline treatment of crystalline ZSM5 can create mesopores by de-silication [48-51]. For our project, 0.2M sodium hydroxide was prepared for the treatment of the parent zeolite to create mesopores. The zeolite and NaOH solution was mixed in a ratio of 1:30 and the solution was maintained at 80°C for 5 hours with continuous stirring using a magnetic stirrer [52]. This mixture was cooled in an ice bath and washed thrice with double distilled water and oven-dried overnight at 85°C for 12 hours. This dried sample was ion-exchanged and calcined following the procedure described in the section 3.5.1. This sample is referred to as Mesoporous zeolite hereby.

### **3.5.3. Acid wash to clean the mesoporous parent zeolite**

In the process of creating mesopores, we suspected we may have blocked some of the micropores with extra framework alumina. To ensure the cleaning of the sample, we

performed acid wash to clean the surface of the mesoporous zeolite. Acid wash of the Mesoporous zeolite was done following the procedure as published in literature [53]. The Mesoporous zeolite sample was washed with 0.2M hydrochloric acid in a ratio of 1:10 at a temperature of 80°C under vigorous stirring for 3 hours. The sample was then washed thrice and oven dried at 85°C for 12 hours. This sample is termed as Acid-Washed Mesopore in the further discussion.

#### 3.5.4. Characterization results of the three zeolites

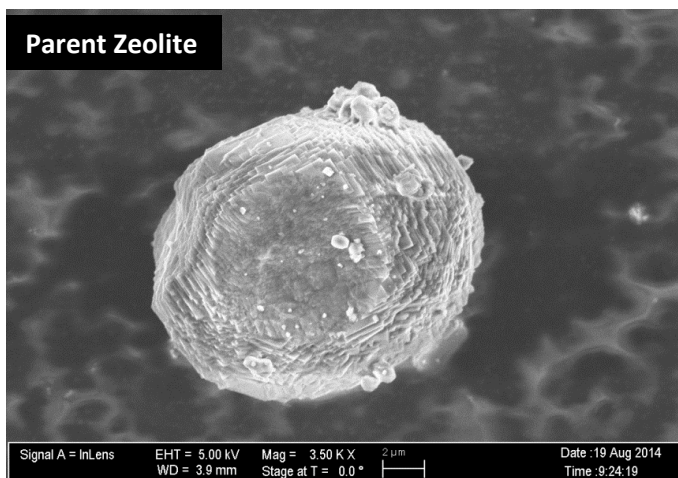


**Figure 26 : SEM of the synthesized parent zeolite sample showing a crystal size of 10 micron**

SEM imaging of the parent zeolite, mesoporous zeolite and acid washed mesopore was performed and the images are shown in figures 26, 27, 28. From the figure 26 the surface of the parent zeolite is relatively uniform and consistent with other ZSM-5 zeolites, the sample has an approximate crystal size of 10  $\mu\text{m}$ .

After attacking the parent zeolite with NaOH, figure 27 shows that the surface is noticeably different. The surface can be seen with pockets and craters indicating that

mesopores may have been created but The spherical form is maintained, implying that the zeolite structure is not collapsed or disturbed, These images are in line with those available in the literature, showing a removal of the interior zeolite[54]. After acid washing, no significant changes were observed to the zeolite structure, as shown in figure 28.

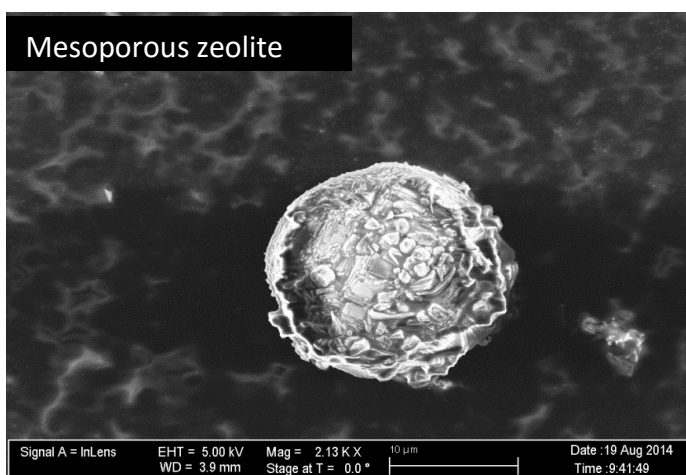


Figure 27: SEM image of the mesoporous zeolite sample



Figure 28 : SEM image of the acid washed mesopore sample



Nitrogen adsorption experiments were performed on the three catalysts to determine the micro-porosity and the mesoporosity and to confirm if the alkaline treatment made any significant changes to the zeolite. The results for the BET experiments are included in Table 2. As we can see in the table, the micropore volume in the mesoporous zeolite is decreased. This can be due to the extra framework alumina blocking few micropores in the zeolite after the NaOH attack. But as we can see, after the acid wash was performed

to remove the extra framework Alumina, the micropore volume returned to the level as seen in the parent zeolite. The mesopore volume and the external surface area followed an increasing trend in the catalyst preparation steps, as expected. The increase in surface area also leads us to believe the zeolite crystal structure was also maintained

	<b>Micropore volume cm<sup>3</sup>/g</b>	<b>Micropore Area cm<sup>2</sup>/g</b>	<b>Total Pore Volume cm<sup>3</sup>/g</b>	<b>Mesopore Volume cm<sup>3</sup>/g</b>	<b>External Surface area m<sup>2</sup>/g</b>
<b>Parent Zeolite</b>	0.186	355	0.222	0.035	19.5
<b>Mesoporous Zeolite</b>	0.165	314.9	0.305	0.140	51.6
<b>Acid-washed mesopore</b>	0.189	361	0.357	0.168	61.0
Measured via t-plot method					

**Table 2: BET results showing micro-porosity, mesoporosity and surface area.**

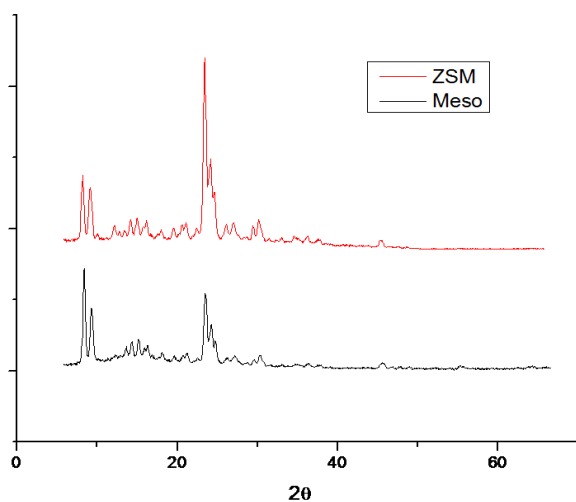


**Figure 29: XRD of the parent zeolite and mesoporous zeolite showing crystallinity**

To further confirm that the crystallinity was maintained after NaOH attack, X-Ray Diffraction (XRD) was performed on the parent and mesopore zeolite catalysts. While a minor loss in crystallinity can be seen in the figure 29, it is evident that the MFI structure of the zeolite was maintained and the XRD patterns agree with what is currently found in literature[55]

IPA-TPD experiment as described in section 2.3.1 was used to determine the Brønsted acid site density of each catalyst and the results are tabulated in the Table 3. The Brønsted acid site density decreased in the mesoporous zeolite sample and it is observed to have increased after the acid washing of the sample. As discussed with the BET results, the hypothesis that we may have blocked some pores with the extra framework alumina subsequent to the NaOH treatment seems to be agreeing with the IPA-TPD results.

	Parent Zeolite	Mesoporous Zeolite	Acid Washed mesopore
<b>Brønsted Acidity (mmol/gm catalyst)</b>	0.189	0.160	0.216
<b>Si/Al ratio</b>	90	103	76
Measured by TPD of Isopropylamine			

**Table 3: IPA-TPD results for the Mesoporous Series of Zeolites**

### 3.5.5. Flow reactions results

The synthesized and modified catalyst samples were used to conduct reactions with hexanoic acid and acetic acid to understand the activity in comparison to the commercial H-ZSM5. The flow reaction studies were performed as described in the section 2.2. The molar ratio of hexanoic acid and acetic acid was maintained at 1: 10, and the reaction temperature at 300°C, with a W/F with respect to acetic acid at 0.095hrs during the reactions. Comparing the activity of the commercial catalyst with the parent zeolite, we expect to see a decrease as the parent zeolite has fewer Brønsted acid sites and a higher Si/Al ratio. Figure 30 shows the turnover frequencies of the two catalysts for co-feeding experiments and it shows a reduced activity in the parent zeolite.

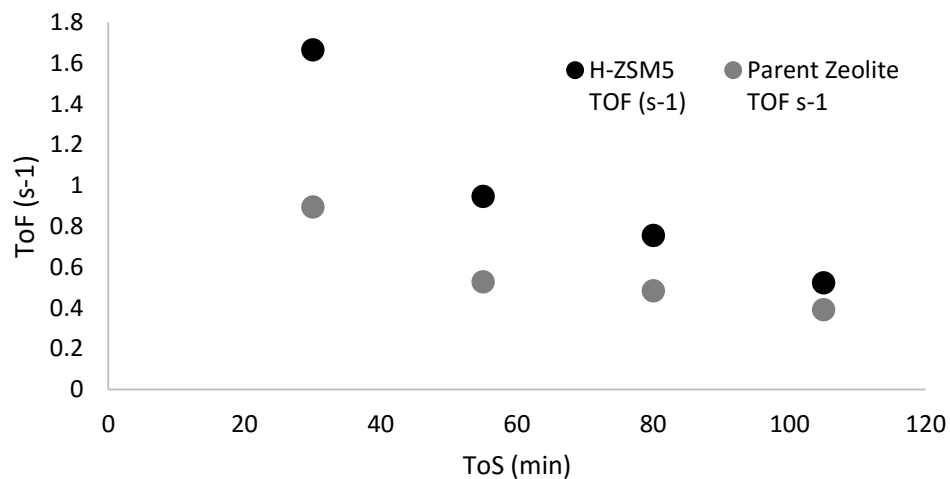


**Figure 30: Turnover frequencies for cross ketone on two different catalysts in co-feeding experiments of hexanoic acid with acetic acid (molar ratio = 1 : 10) at T=300C**

Figure 31 shows the comparison of the activity of the three catalysts, the parent zeolite, the mesoporous zeolite and the acid washed mesopore samples of the co-feeding hexanoic acid with acetic acid reaction at the same reaction conditions. It is observed that the acid washed zeolite has a much better activity compared to the other zeolites, due to the removal of probable pore blockage while creating mesopores. The mesoporous zeolite, though has a higher activity than the parent zeolite, it is lower than the activity on the acid washed mesopore sample. The parent zeolite has the lowest number of Brønsted acid sites, therefore has the lowest activity. The carbon balances were calculated to be above 90%.

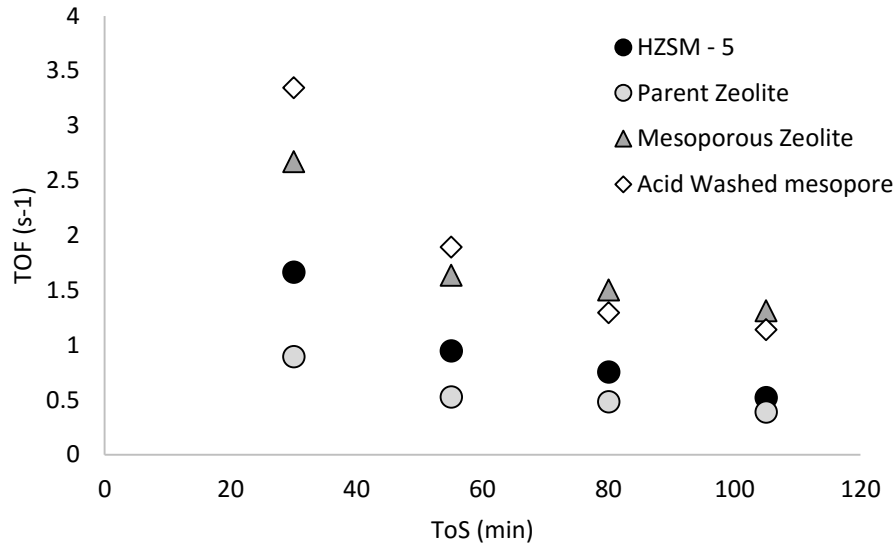


**Figure 31: Turnover frequencies of mesoporous series based on conversion of hexanoic acid co fed with acetic acid to a cross ketone at T=300C and same conditions compared to commercial H-ZSM5**

This confirms the hypothesis that shorter diffusion path yields higher amounts of the cross ketone on H-ZSM5 catalyst.

### 3.6. Succinic acid

The idea of forming a cross ketone on H-ZSM5 can be of significant interest for application in the biomass feed. Work in our group indicated that succinic acid can be formed by oxidation of furfural over Amberlyst -15 catalyst.

Succinic acid is a dicarboxylic acid containing two acid functional groups. Attempts were made to perform ketonization reaction of the succinic acid over H-ZSM5 in a flow reaction set up as described in section 2.2. Different solvents were used for making a

solution with succinic acid. Table 4 indicates the solvents that were used to attempt vapor phase reactions with succinic acid at different temperatures.

<b>Solvent</b>	<b>Mole ratio</b>	<b>Reaction Temperature</b>	<b>Products Observed</b>
<b>Acetic Acid</b>	1:200	300	none
	1: 120	350	none
<b>Acetonitrile</b>	1: 170	300	none
<b>Water</b>	1: 500	300	none

**Table 4: Table showing various solvents, molar ratios and temperatures used for succinic acid flow reactions**

The succinic acid seemed to be very difficult to work with in the vapor phase reaction. Also a temperature programmed desorption study indicated that the succinic acid solution made with the solvent acetic acid may not be undergoing any reaction on H-ZSM5 surface., figure shows mass spectrum for masses 55, 74 and 100 pertaining to succinic acid. This shows that the succinic acid may not have reached the catalyst bed.

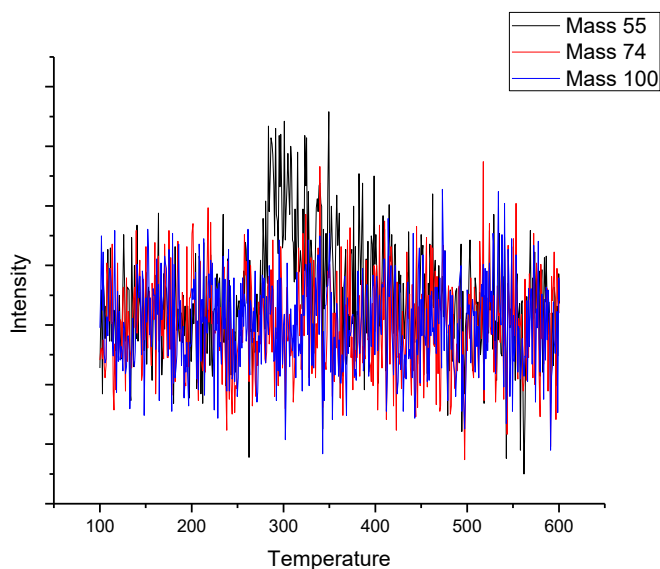


**Figure 32: TPD results of succinic acid on H-ZSM5 with acetic acid as solvent**

Therefore, further studies could not be conducted for ketonization reaction of succinic acid in my reaction system. For future studies, possibility of a bubbler being used for vaporizing the succinic acid to reach the catalyst bed.

### **3.7. Furoic acid**

Work from our group indicated that selective oxidation of furfural can produce 2-furoic acid over synthesized gold supported on MgO catalyst. Furfural is one of the most abundant species in bio-mass Torrefaction streams, 2- furoic acid ketonization can be a reaction of importance if it can make cross ketones with acetic acid which is also abundant in the bio mass streams.

As furoic acid is a crystalline solid, in a mole ratio of 1:23 acetic acid was used as solvent to make a solution mixture. To examine this reaction, furoic acid was fed into the vapor

phase reactor described in section 2.2. At a reaction temperature of 300°C on H-ZSM5 catalyst, no products were observed.

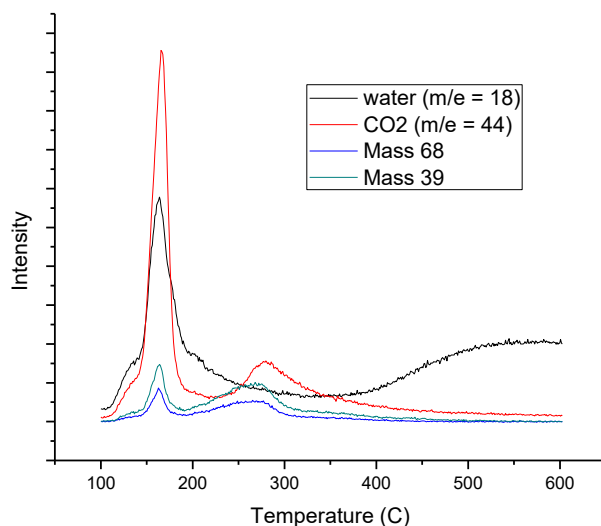


**Figure 33: TPD results of 2-Furoic acid over H-ZSM5 with acetic acid as solvent**

To understand furoic acid reaction on the surface of a catalyst, a TPD experiment was performed with the mixture as described in section 2.3.2 and figure 33 shows the mass spectra of water, CO<sub>2</sub> and furan. The color of the mixture does not change with time showing that the mixture of 2-furoic acid and acetic acid is stable.

This indicates that the furoic acid is decomposing into furan suggesting that vapor phase experiments with 2-furoic acid over H-ZSM5 catalyst are difficult and not a good path forward as furoic acid seems to be decomposing.



#### 4. Chapter 4: Conclusions

Similar to acetic acid ketonization mechanism benzoic acid dehydrates to form surface acyl over H-ZSM5 but does not couple with a second benzoic acid molecule to form self-ketone. Instead benzoic acid produces a cross ketone when co-fed with acetic acid which emphasizes the importance of alpha hydrogen for the second carboxylic acid. Since benzoic acid can form surface acyls, it suggests that acyl can be formed with or without alpha hydrogen and this hypothesis is supported by  $^{13}\text{C}$  labelled experiments.

Ready decomposition of pivalic acid at a very low temperature did not seem promising for further studying the mechanism. However, pivalic acid reversibly inhibits the ketonization activity of acetic acid on HZSM-5.

Stability of surface acyl was observed to be increasing with increase in carbon chain length as suggested by propionic acid and hexanoic experiments when co-fed with acetic acid. Steric effects from surface adsorbed long carbon acyl inside the confinement may be favoring C-C coupling with the tautomer from a smaller carbon chain acid. This hypothesis is believed to be the reason for high selectivity towards cross ketone.

Mesoporous catalyst exhibit better activity and stability by reducing diffusion length in desorption of bulkier ketones.

## 5. References

1. Barrow, M.P., et al., *Determination of the nature of naphthenic acids present in crude oils using nanospray Fourier transform ion cyclotron resonance mass spectrometry: The continued battle against corrosion*. Analytical chemistry, 2003. **75**(4): p. 860-866.
2. Zhang, A., et al., *Improved processes to remove naphthenic acids*. Annual Technical Progress Report, California Institute of Technology, 2005: p. 1-24.
3. Zhang, A., et al., *Naphthenic acid removal from crude oil through catalytic decarboxylation on magnesium oxide*. Applied Catalysis A: General, 2006. **303**(1): p. 103-109.
4. Quiroga-Becerra, H., et al., *A kinetic study of esterification of naphthenic acids from a Colombian heavy crude oil*. CT&F-Ciencia, Tecnología y Futuro, 2012. **4**(5): p. 21-31.
5. McKendry, P., *Energy production from biomass (part 1): overview of biomass*. Bioresource technology, 2002. **83**(1): p. 37-46.
6. Czernik, S. and A. Bridgwater, *Overview of applications of biomass fast pyrolysis oil*. Energy & Fuels, 2004. **18**(2): p. 590-598.
7. Huber, G.W., S. Iborra, and A. Corma, *Synthesis of transportation fuels from biomass: chemistry, catalysts, and engineering*. Chemical reviews, 2006. **106**(9): p. 4044-4098.
8. Huber, G.W. and A. Corma, *Synergies between Bio-and Oil Refineries for the Production of Fuels from Biomass*. Angewandte Chemie International Edition, 2007. **46**(38): p. 7184-7201.

9. Goyal, H., D. Seal, and R. Saxena, *Bio-fuels from thermochemical conversion of renewable resources: a review*. Renewable and Sustainable Energy Reviews, 2008. **12**(2): p. 504-517.
10. Kumar, A., D.D. Jones, and M.A. Hanna, *Thermochemical biomass gasification: a review of the current status of the technology*. Energies, 2009. **2**(3): p. 556-581.
11. Mortensen, P.M., et al., *A review of catalytic upgrading of bio-oil to engine fuels*. Applied Catalysis A: General, 2011. **407**(1): p. 1-19.
12. Zhang, Q., et al., *Review of biomass pyrolysis oil properties and upgrading research*. Energy conversion and management, 2007. **48**(1): p. 87-92.
13. Kim, K. and M. Barteau, *Structure and composition requirements for deoxygenation, dehydration, and ketonization reactions of carboxylic acids on TiO<sub>2</sub> (001) single-crystal surfaces*. Journal of Catalysis, 1990. **125**(2): p. 353-375.
14. Doornkamp, C. and V. Ponc, *The universal character of the Mars and Van Krevelen mechanism*. Journal of Molecular Catalysis A: Chemical, 2000. **162**(1): p. 19-32.
15. DEMİRBAŞ, A., *Hydrocarbons from pyrolysis and hydrolysis processes of biomass*. Energy sources, 2003. **25**(1): p. 67-75.
16. Martinez, R., M. Huff, and M. Barteau, *Ketonization of acetic acid on titania-functionalized silica monoliths*. Journal of Catalysis, 2004. **222**(2): p. 404-409.
17. Alonso, D.M., J.Q. Bond, and J.A. Dumesic, *Catalytic conversion of biomass to biofuels*. Green Chemistry, 2010. **12**(9): p. 1493-1513.
18. Snell, R.W. and B.H. Shanks, *Insights into the ceria-catalyzed ketonization reaction for biofuels applications*. ACS Catalysis, 2013. **3**(4): p. 783-789.

19. Pestman, R., et al., *Reactions of carboxylic acids on oxides: 1. Selective hydrogenation of acetic acid to acetaldehyde*. Journal of catalysis, 1997. **168**(2): p. 255-264.
20. Pestman, R., et al., *Reactions of carboxylic acids on oxides: 2. Bimolecular reaction of aliphatic acids to ketones*. Journal of catalysis, 1997. **168**(2): p. 265-272.
21. Pham, T.N., et al., *Ketonization of carboxylic acids: mechanisms, catalysts, and implications for biomass conversion*. ACS Catalysis, 2013. **3**(11): p. 2456-2473.
22. Pham, T.N., D. Shi, and D.E. Resasco, *Evaluating strategies for catalytic upgrading of pyrolysis oil in liquid phase*. Applied Catalysis B: Environmental, 2014. **145**: p. 10-23.
23. Zapata, P.A., et al., *Condensation/hydrogenation of biomass-derived oxygenates in water/oil emulsions stabilized by nanohybrid catalysts*. Topics in Catalysis, 2012. **55**(1-2): p. 38-52.
24. Pham, T.N., D. Shi, and D.E. Resasco, *Kinetics and mechanism of ketonization of acetic acid on Ru/TiO<sub>2</sub> catalyst*. Topics in Catalysis, 2014. **57**(6-9): p. 706-714.
25. Renz, M., *Ketonization of carboxylic acids by decarboxylation: mechanism and scope*. European journal of organic chemistry, 2005. **2005**(6): p. 979-988.
26. Izumi, J., et al., *Handbook of Zeolite Science and Technology*. 2003, Marcel Dekker New York.
27. Argauer, R.J. and G.R. Landolt, *Crystalline zeolite ZSM-5 and method of preparing the same*. 1972, Google Patents.
28. Weitkamp, J., *Zeolites and catalysis*. Solid State Ionics, 2000. **131**(1): p. 175-188.
29. Baerlocher, C., L.B. McCusker, and D.H. Olson, *Atlas of zeolite framework types*. 2007: Elsevier.

30. Pestman, R., et al., *The formation of ketones and aldehydes from carboxylic acids, structure-activity relationship for two competitive reactions*. Journal of molecular catalysis A: chemical, 1995. **103**(3): p. 175-180.
31. Rand, L., et al., *Reactions Catalyzed by Potassium Fluoride. II. The Conversion of Adipic Acid to Cyclopentanone*. The Journal of Organic Chemistry, 1962. **27**(3): p. 1034-1035.
32. Libby, M.C., P.C. Watson, and M.A. Barteau, *Synthesis of Ketenes with oxide catalysts*. Industrial & engineering chemistry research, 1994. **33**(12): p. 2904-2912.
33. Pulido, A., et al., *Ketonic decarboxylation reaction mechanism: a combined experimental and DFT study*. ChemSusChem, 2013. **6**(1): p. 141-151.
34. Vervecken, M., et al., *Zeolite-induced selectivity in the conversion of the lower aliphatic carboxylic acids*, in *Chemical Reactions in Organic and Inorganic Constrained Systems*. 1986, Springer. p. 95-114.
35. Martens, J., et al., *Acid-catalyzed ketonization of mixtures of low carbon number carboxylic acids on zeolite HT*. Studies in Surface Science and Catalysis, 1993. **78**: p. 527-534.
36. Chang, C., et al., *Synergism in acetic acid/methanol reactions over ZSM-5 zeolites*. Prepr. Pap.-Am. Chem. Soc., Div. Fuel Chem.:(United States), 1983. **28**(CONF-830303-).
37. Chiche, B., et al., *Friedel-Crafts acylation of toluene and p-xylene with carboxylic acids catalyzed by zeolites*. The Journal of Organic Chemistry, 1986. **51**(11): p. 2128-2130.
38. Bonati, M.L., R.W. Joyner, and M. Stockenhuber, *A temperature programmed desorption study of the interaction of acetic anhydride with zeolite beta (BEA)*. Catalysis today, 2003. **81**(4): p. 653-658.

39. Bonati, M.L., R.W. Joyner, and M. Stockenhuber, *On the mechanism of aromatic acylation over zeolites*. Microporous and mesoporous materials, 2007. **104**(1): p. 217-224.
40. Gumidyala, A.S., T.; and Crossley, S. submitted, . , 2016.
41. Escola, J. and M. Davis, *Acylation of biphenyl with acetic anhydride and carboxylic acids over zeolite catalysts*. Applied Catalysis A: General, 2001. **214**(1): p. 111-120.
42. Fogler HS, *Elements of chemical reaction engineering, chapter 10–12, 2005, 4th edn. Prentice Hall Publisher, Englewood Cliffs.*
43. Hoang, T.Q., et al., *Effects of HZSM-5 crystallite size on stability and alkyl-aromatics product distribution from conversion of propanal*. Catalysis Communications, 2010. **11**(11): p. 977-981.
44. Armaroli, T., et al., *Effects of crystal size and Si/Al ratio on the surface properties of H-ZSM-5 zeolites*. Applied Catalysis A: General, 2006. **306**: p. 78-84.
45. Li, J., et al., *Catalytic fast pyrolysis of biomass with mesoporous ZSM-5 zeolites prepared by desilication with NaOH solutions*. Applied Catalysis A: General, 2014. **470**: p. 115-122.
46. Bjørgen, M., et al., *Methanol to gasoline over zeolite H-ZSM-5: Improved catalyst performance by treatment with NaOH*. Applied Catalysis A: General, 2008. **345**(1): p. 43-50.
47. Zhu, X., et al., *Tailoring the mesopore structure of HZSM-5 to control product distribution in the conversion of propanal*. Journal of Catalysis, 2010. **271**(1): p. 88-98.
48. Van Donk, S., et al., *Generation, characterization, and impact of mesopores in zeolite catalysts*. Catalysis Reviews, 2003. **45**(2): p. 297-319.

49. Groen, J., et al., *On the introduction of intracrystalline mesoporosity in zeolites upon desilication in alkaline medium*. *Microporous and Mesoporous Materials*, 2004. **69**(1): p. 29-34.
50. Groen, J.C., J.A. Moulijn, and J. Pérez-Ramírez, *Desilication: on the controlled generation of mesoporosity in MFI zeolites*. *Journal of Materials Chemistry*, 2006. **16**(22): p. 2121-2131.
51. Verboekend, D. and J. Pérez-Ramírez, *Design of hierarchical zeolite catalysts by desilication*. *Catalysis Science & Technology*, 2011. **1**(6): p. 879-890.
52. Ogura, M., et al., *Formation of Uniform Mesopores in ZSM-5 Zeolite through Treatment in Alkaline Solution*. *Chemistry letters*, 2000(8): p. 882-883.
53. Caicedo-Realpe, R. and J. Pérez-Ramírez, *Mesoporous ZSM-5 zeolites prepared by a two-step route comprising sodium aluminate and acid treatments*. *Microporous and mesoporous materials*, 2010. **128**(1): p. 91-100.
54. Dessau, R., E. Valyocsik, and N. Goeke, *Aluminum zoning in ZSM-5 as revealed by selective silica removal*. *Zeolites*, 1992. **12**(7): p. 776-779.
55. Wu, E., et al., *ZSM-5-type materials. Factors affecting crystal symmetry*. *Journal of Physical Chemistry*, 1979. **83**(21): p. 2777-2781.